Plant, Cell & Environment

WILEY

Plant, Cell & Environment

ORIGINAL ARTICLE

Tyrosylprotein Sulfotransferase Positively Regulates Symbiotic Nodulation and Root Growth

Danping Zhang[1] | Qi Di[1] | Jinshan Gui[2] | Qiong Li[1] | Kirankumar S. Mysore[3] | Jiangqi Wen[3] | Li Luo[1] | Liangliang Yu[1,2]

[1]Shanghai Key Laboratory of Bio-Energy Crops, School of Life Sciences, Shanghai University, Shanghai, China | [2]State Key Laboratory of Subtropical Silviculture, Zhejiang A&F University, Hangzhou, Zhejiang, China | [3]Institute for Agricultural Biosciences, Oklahoma State University, Ardmore, Oklahoma, USA

Correspondence: Liangliang Yu (yuliangliang@shu.edu.cn)

Received: 18 December 2023 | **Revised:** 29 August 2024 | **Accepted:** 30 August 2024

Funding: This study was supported by National Natural Science Foundation of China and State Key Laboratory of Subtropical Silviculture (Grants 31500197 and SKLSS-KF2023-01).

Keywords: *Medicago truncatula* | PSK | RGF | root growth | symbiotic nodulation | tyrosylprotein sulfotransferase

ABSTRACT

Posttranslational tyrosine sulfation of peptides and proteins is catalysed by tyrosylprotein sulfotransferases (TPSTs). In *Arabidopsis*, tyrosine sulfation is essential for the activities of peptide hormones, such as phytosulfokine (PSK) and root meristem growth factor (RGF). Here, we identified a TPST-encoding gene, *MtTPST*, from model legume *Medicago truncatula*. *MtTPST* expression was detected in all organs, with the highest level in root nodules. A *promoter:GUS* assay revealed that *MtTPST* was highly expressed in the root apical meristem, nodule primordium and nodule apical meristem. The loss-of-function mutant *mttpst* exhibited a stunted phenotype with short roots and reduced nodule number and size. Application of both of the sulfated peptides PSK and RGF3 partially restored the defective root length of *mttpst*. The reduction in symbiotic nodulation in *mttpst* was partially recovered by treatment with sulfated PSK peptide. MtTPST-PSK module functions downstream of the Nod factor signalling to promote nodule initiation via regulating accumulation and/or signalling of cytokinin and auxin. Additionally, the small-nodule phenotype of *mttpst*, which resulted from decreased apical meristematic activity, was partially complemented by sulfated RGF3 treatment. Together, these results demonstrate that MtTPST, through its substrates PSK, RGF3 and other sulfated peptide(s), positively regulates nodule development and root growth.

1 | Introduction

Legumes interact with *Rhizobium* bacteria to form an organ called the root nodule, in which rhizobia convert atmospheric dinitrogen to ammonia to support host plant growth and improve soil fertility (Ferguson et al. 2019). Root nodule formation requires spatiotemporal orchestration of two developmental processes: rhizobial infection and nodule organogenesis (Oldroyd et al. 2011). In the model legume *Medicago truncatula*, the microsymbiont *Sinorhizobium meliloti* enters the epidermis via a curled root hair and penetrates into cortical cells via an infection thread (IT) (Jones et al. 2007). Simultaneously, the middle and inner cortex, endodermis and pericycle of the host roots dedifferentiate and divide to form a nodule primordium (Xiao et al. 2014). ITs progress into the nodule primordium and release rhizobia in a membrane-enclosed form called a symbiosome (Mohd-Radzman and Drapek 2023). The rhizobia in symbiosomes subsequently differentiate into bacteroids and begin to fix nitrogen (Oldroyd et al. 2011).

Initiation of both programmes of rhizobial infection and nodule organogenesis in *M. truncatula* root cells depends on the

Danping Zhang and Qi Di contributed equally to this study.

perception of rhizobia-secreted nodulation factors (NFs) by LysM receptor-like kinases (LYK3 and NFP) (Limpens et al. 2003; Oldroyd 2013). These NF receptors induce calcium oscillations in the nucleus via a set of proteins. Calcium signals are further decoded by the calcium-activated kinase DMI3, which phosphorylates IPD3. Phosphorylated IPD3 interacts with DELLAs and NSP1/2 to activate expression of core symbiotic transcription factors, such as NIN and ERNs (Oldroyd 2013; Yang et al. 2022). Recently, Dong et al. (2021) reported that a cortical SHR-SCR module functions downstream of the NF signalling pathway to regulate nodule organogenesis. Typical legume nodules are classified into two types: indeterminate and determinate. *M. truncatula* produces indeterminate nodules, which have a persistent meristem in the apical region. The meristem divides and differentiates to generate new cells for bacterial internalization, thereby controlling indeterminate nodule growth (Yang et al. 2022). According to a detailed study of the developmental process of indeterminate nodules, the apical meristem arises from the middle cortex of roots (Xiao et al. 2014); however, the regulatory mechanism controlling meristem growth and nodule elongation remains unclear.

Since the first identification of systemin from tomato leaves (Pearce et al. 1991), dozens of peptide hormones have been discovered to play important roles in plants. Among them, several peptide hormones require tyrosine sulfation to achieve full activity (Matsubayashi 2011). Tyrosine sulfation is a post-translational modification catalysed by tyrosylprotein sulfotransferase (TPST). This enzyme catalyses the transfer of sulfate from the cosubstrate 3′-phosphoadenosine 5′-phosphosulfate (PAPS) to the phenolic group of tyrosine (Moore 2003; Ma et al. 2023). Plant TPST activities were first identified from microsomal fractions of several plant cell lines, and the presence of an aspartic acid residue adjacent to the first tyrosine residue was confirmed to be essential for the sulfation reaction (Hanai et al. 2000). *Arabidopsis AtTPST* is the first TPST-encoding gene to be cloned and characterized, and the deduced protein is a 500-amino acid type I transmembrane protein localized to the *cis*-Golgi, where sulfation occurs (Komori et al. 2009). *AtTPST* is a single-copy gene in *Arabidopsis* and ubiquitously expressed, with the highest level in the root apical meristem (Komori et al. 2009). Loss-of-function mutants of *AtTPST* (*tpst-1*/*aqc1-2*, *aqc1-1*, *sgn2*) display multiple defects, such as dwarfism, short roots, early senescence, reduced fertility (Komori et al. 2009; Zhou et al. 2010), defective Casparian strip formation (Doblas et al. 2017) and altered immune responses (Igarashi, Tsuda, and Katagiri 2012; Mosher et al. 2013).

As a single-copy gene, *AtTPST* mutation resulted in a broad range of phenotypes, suggesting a critical role in synthesizing all tyrosine-sulfated peptides in *Arabidopsis*. To date, four classes of tyrosine-sulfated peptides have been reported in plants: phytosulfokine (PSK), root meristem growth factor (RGF)/GOLVEN/CLE-like (CLEL), plant peptide-containing sulfated tyrosine (PSY) and Casparian strip integrity factor (CIF) (Kaufmann and Sauter 2019).

The first identified sulfated peptide hormone was PSK, which is a secreted pentapeptide harbouring two sulfated tyrosines. PSK-α, with the sequence $Y_{SO_3}IY_{SO_3}TQ$, was initially identified as a key chemical inducer involved in promoting division of cells cultured at low density (Matsubayashi and Sakagami 1996) and was later found to play multiple roles in plant growth, development and stress resistance (Sauter 2015; Li et al. 2024). PSK peptides are generated from approximately 100-amino acid-long precursors (Yang et al. 2001; Lorbiecke and Sauter 2002) containing an N-terminal signal peptide for secretory pathway targeting and the PSK pentapeptide sequence near the C-terminus (Sauter 2015). Maturation of PSK peptides from precursors occurs through TPST-catalysed tyrosine sulfation in the *cis*-Golgi (Komori et al. 2009) and subsequent proteolytic cleavage executed by subtilisin proteases in the apoplast (Reichardt et al. 2020; Stührwohldt et al. 2021). PSK peptides bind to leucine-rich repeat receptor kinase PSKRs on the plasma membrane (Matsubayashi et al. 2002), stabilizing PSKR island domains for recruitment of the coreceptor BAK1 (Ladwig et al. 2015; Wang, Li, et al. 2015) and forming a module with CNGC17 and H^+-ATPases to transduce signals (Ladwig et al. 2015).

Our previous studies in *Lotus japonicus* found that two PSK-α-encoding genes, *LjPSK1* and *LjPSK4*, are expressed specifically in root nodules. Overexpression of *LjPSK1* or external application of PSK-α peptide increases nodule number (Wang, Yu, et al. 2015). Recently, we identified two novel types of PSKs, PSK-δ ($Y_{SO_3}IY_{SO_3}TN$) and PSK-ε ($Y_{SO_3}VY_{SO_3}TN$), specifically from legume species. In *M. truncatula*, the PSK-δ precursor gene *MtPSKδ* is highly expressed in nodule primordia, young nodules and the apical region of mature nodules. Both overexpression of *MtPSKδ* and treatment with PSK-δ peptide enhance nodule organogenesis (Yu et al. 2022). In addition, PSK-ε promotes symbiotic nodulation and root development in *M. truncatula* (Di et al. 2022). These findings indicate that different types of PSK peptides, including PSK-α, PSK-δ and PSK-ε, synergistically regulate nodule formation in legumes.

RGF peptides were initially identified by a search for sulfated peptides involved in recovery of the defective root growth of the *tpst-1* mutant. The *tpst-1* exhibits a short root phenotype with significantly decreased apical meristematic activity (Matsuzaki et al. 2010; Zhou et al. 2010). The previously identified sulfated peptides PSK and PSY1 were only able to partially rescue the *tpst-1* root phenotype through root cell elongation promotion, and application of the RGF1 peptide restored root meristematic activity (Matsuzaki et al. 2010). RGFs are 13-amino acid-long peptides that mature from their precursors through tyrosine sulfation catalysed by TPST and proteolytic cleavage executed by subtilases, including SBT6.1 (Ghorbani et al. 2016). In *Arabidopsis*, RGFs are encoded by a gene family that consists of 10 precursor genes (Shinohara 2021). Expression profile analyses have revealed that most of these genes are transcribed in roots, with five being expressed in the root apical meristem (Fernandez et al. 2013). Similar to *tpst-1*, the *rgf1/2/3* triple mutant has a small root apical meristem, which can be reversed by RGF1 treatment (Matsuzaki et al. 2010). Recently, three research groups have independently identified RGF receptors, namely, RGFRs/RGIs (Ou et al. 2016; Shinohara et al. 2016; Song et al. 2016). Binding of RGFs by receptors controls the distribution of reactive oxygen species (ROS) in roots by inducing expression of *RGF1 inducible transcription factor 1* (*RITF1*); ROS redistribution in turn enhances the stability of

PLETHORA (PLT) proteins, which are master regulators of the maintenance of root stem cells (Zhou et al. 2010; Ou et al. 2016; Shinohara et al. 2016; Yamada, Han, and Benfey 2020). In addition to its function in the root apical meristem, RGF signalling controls root gravitropism (Meng et al. 2012; Whitford et al. 2012), lateral root formation (Meng et al. 2012; Fernandez et al. 2015, 2020), root hair development (Fernandez et al. 2013) and innate immunity (Wang et al. 2021). Recently, Li et al. (2020) identified a rhizobium-inducible RGF gene, *MtRGF3*, in *M. truncatula* and found that the MtRGF3 peptide negatively regulates nodulation.

The other two classes of tyrosine-sulfated peptides are PSYs and CIFs. PSY peptides comprise 14–21 amino acids and derive from precursors, which are encoded by nine genes in *Arabidopsis* (Ogawa-Ohnishi et al. 2022). Similar to PSKs, PSY1 peptide promotes cell proliferation and expansion in plants (Amano et al. 2007). A recent study revealed that receptor-mediated PSY signalling regulates the trade-off between plant growth and stress resistance (Ogawa-Ohnishi et al. 2022). CIF1 and CIF2 are tyrosine-sulfated 21-amino acid peptides to rescue the root Casparian strip defects of *AtTPST* mutants. CIF1/2 peptides are generated in the root stele and specifically bind the endodermis-expressed receptors GSO1/SGN3 and GSO2 to control contiguous Casparian strip formation (Doblas et al. 2017; Nakayama et al. 2017). Interestingly, two different types of sulfated peptides, CIF2 and PSY1, both released from the endosperm, act synergistically to promote seedling cuticle formation in *Arabidopsis* (De Giorgi et al. 2021). More recently, Okuda et al. (2020) identified another two CIFs, CIF3 and CIF4, which trigger GSO-dependent signalling to promote pollen wall formation (Truskina et al. 2022).

In this study, we identified and characterized a single TPST-encoding gene, *MtTPST,* from *M. truncatula*. *MtTPST* is highly expressed in the root apical meristem, lateral root primordium, nodule primordium and nodule apical meristem. The *mttpst* mutant exhibits stunted growth with short roots and reduced nodule number and size. Sulfated PSK and RGF3 peptides, together or in each application, partially restored the defective phenotype of *mttpst*, suggesting that MtTPST promotes nodule formation and root growth through its substrate peptides.

2 | Materials and Methods

2.1 | Plant Material and Growth Conditions

The *M. truncatula* ecotype Jemalong A17 and the nodulation mutants *nfp*, *dmi3*, *nsp1* and *nin* were used for *MtTPST* expression pattern analyses. A17 was also employed for hairy root transformation. The *Tnt1*-insertion mutants (R108 background) were purchased from the Samuel Roberts Nobel Foundation *M. truncatula* mutant library. The *MtTPST* loss-of-function mutant *mttpst* was used for stable genetic transformation. *M. truncatula* seeds were scarified for 6 min in H_2SO_4 followed by sterilization for 4 min with 10% (v/v) NaClO. Sterilized seeds were stratified on 1% agar plates for 2 days and then germinated in the dark overnight at 23°C. Germinated seedlings were planted to pots containing a 3:1 ratio of vermiculite:perlite supplied with half-strength Fahraeus medium. *Arabidopsis thaliana* ecotype Columbia (Col-0) and the *tpst-1* mutant (SALK_009847, obtained from *Arabidopsis* biological resource centre) seeds were surface-sterilized for 10 min in 5% (v/v) NaClO and then rinsed three times with sterilized water. These seeds were germinated and grown on Murashige and Skoog (MS) medium or in soil. Both *M. truncatula* and *Arabidopsis* were cultured in a greenhouse at 23°C with 50% relative humidity and a 16/8 h light/dark cycle.

2.2 | Bacterial Strains

For *M. truncatula* symbiotic phenotype analyses, seedlings were inoculated with the *Sinorhizobium meliloti* 2011 strain ($OD_{600} = 0.02$). For infection thread and nodule primordium observation, the *S. meliloti* 1021 strain containing the *pXLGD4* plasmid was inoculated. *Agrobacterium tumefaciens* strain EHA105 and *Agrobacterium rhizogenes* strain Arqua1 were used for *M. truncatula* stable genetic transformation and hairy root transformation, respectively. *A. tumefaciens* strain GV3101 was used for *Arabidopsis* genetic transformation.

2.3 | Plasmid Construction

The *MtTPST* CDS was polymerase chain reaction (PCR) amplified using cDNA reverse-transcribed from *M. truncatula* (A17) nodule RNA. The obtained CDS was cloned and inserted into the binary vector pCambia1300-GFP downstream of the enhanced cauliflower mosaic virus (CaMV) 35S promoter using the homologous recombination method (ClonExpress II One step Cloning kit; Vazyme, Nanjing, China). The resulting *35S:MtTPST* overexpressing plasmid was transformed into *M. truncatula* hairy roots, and transgenic lines were selected by observation of GFP fluorescence. For *pMtTPST:GUS* construction, the 2405-bp region upstream of the *MtTPST* coding sequence, considered the promoter (Table S2), was PCR cloned from A17 genomic DNA, and the 35S promoter of the pBI121 vector was replaced using the *Hind* III and *Bam*H I restriction sites. To construct the *pMtTPST:MtTPST* complementation vector, the 35S promoter of the *35S:MtTPST* plasmid was replaced by the *MtTPST* promoter, which is of the same sequence with that used for *pMtTPST:GUS* plasmid, using the *Kpn* I and *Cla* I restriction sites. For *pAtTPST:MtTPST* construction, the 2005-bp promoter upstream of the *AtTPST* coding sequence (Table S2) was PCR cloned from *Arabidopsis* (Col-0) genomic DNA, and the *MtTPST* promoter of *pMtTPST:MtTPST* plasmid was replaced with the *Kpn* I and *Asc* I restriction sites. All restriction enzymes were purchased from Thermo Fisher (Waltham, MA, USA). The primers used are listed in Table S3.

2.4 | Plant Transformation

Stable genetic transformation of *pMtTPST:MtTPST* into *mttpst* mutant was performed according to an established procedure (Yu et al. 2022). In brief, the construct was transferred into the *A. tumefaciens* EHA105 strain and cultured in YEB liquid medium supplemented with 50 mg/L kanamycin and 50 mg/L rifampicin. The agrobacterium was then collected and

resuspended in SH3a liquid medium. Leaflets of *M. truncatula* R108 plants were sterilized in 8% commercial bleach and subsequently cut into square pieces before placed into the above agrobacteria mixture. Next, the leaf explants were transferred to solid SH3a medium (Cosson et al. 2006) for 2 days in the dark. Then the explants were transferred to new SH3a medium and cultured for 6 weeks in the dark to induce callus formation. The GFP-positive calli examined under a SMZ18 fluorescence stereomicroscope (Nikon, Tokyo, Japan) were transferred to new SH3a medium every 2 weeks. These calli were further transferred to hormone-free SH9 medium to induce embryogenesis and plantlet development. Finally, the plantlets were transferred to 1/2 SH9 medium to induce rooting.

For hairy root transformation of *35S:MtTPST* in *M. truncatula* A17, the construct was introduced into *A. rhizogenes* strain Arqua1, and transformation was performed according to a reported method (Boisson-Dernier et al. 2001).

2.5 | Peptide Treatment

The PSK-α ($Y_{SO3}IY_{SO3}TQ$), RGF3 [DY_{SO3}SPARKKS(Hyp)IHN], desulfated (ds) PSK-α (YIYTQ) and dsRGF3 [DYSPARKKS(Hyp) IHN] peptides were chemically synthesized by Chinese Peptide Company (Hangzhou, China) with the purity greater than 96%. Each peptide was dissolved in sterilized ddH_2O with a concentration of 1 mM, which was used as the stock solution and kept at −80°C before use. For root growth comparison, germinated seedlings of *M. truncatula* were planted in autoclaved soil that was soaked with 1 μM peptides. For symbiotic nodulation, *M. truncatula* seedlings grown in autoclaved soil were inoculated with *S. meliloti* 2011 and irrigated with 1 μM peptides every 4 days.

2.6 | Nitrogenase Activity

The nitrogenase activity of nodules was determined by the acetylene reduction assay. Nodules detached from five *M. truncatula* plants were incubated with 0.5 mL acetylene in a sealed vial (5 mL in volume) at 28°C for 1 h. The produced ethylene was measured with a GC-7900 gas chromatograph (Techcomp, Shanghai, China).

2.7 | RNA Extraction and Quantitative Reverse Transcription-PCR (qRT-PCR)

Total RNA was isolated with the RNAprep pure Plant kit (Tiangen, Beijing, China) according to the manufacturer's instructions. After DNase treatment, the RNA was quantified with a Nanodrop spectrophotometer (Thermo Fisher, Waltham, MA, USA). RNA (1 μg) was used for cDNA synthesis using the HiScript II Q-RT Supermix kit (Vazyme, Nanjing, China). The samples were diluted 30 times before use. The qRT-PCR experiments were done on a CFX96 real-time PCR detection system (Bio-Rad, Hercules, CA, USA), and Hieff qPCR SYBR Green Master Mix (Yeasen, Shanghai, China) was used for detection. The PCR procedure and data analysis ($\Delta\Delta C_t$ method) were described in a previous study (Yu et al. 2014). The relative expression of *MtTPST* gene was normalized against the housekeeping gene *MtActinB*. The gene-specific primers used for qRT-PCR are listed in Table S3.

2.8 | RNA-Sequencing

Wild-type *M. truncatula* (R108) and *mttpst* mutant seedlings at 5-day old were inoculated with *S. meliloti* 2011 for 24 h, and the root samples were collected for RNA-sequencing (RNA-seq). Total RNA was extracted from three independent wild-type and *mttpst* samples. Paired-end sequencing libraries were created and sequenced by Majorbio Bio-pharm Technology Company (Shanghai, China) on Illumina NovaSeq X Plus platform. The raw reads were filtered to generate clean reads and then mapped to the *M. truncatula* genome (MedtrA17_4.0, http://plants.ensembl.org/Medicago_truncatula/Info/Index). The mapping rates of the wild type and *mttpst* were 86.5% and 87.2%, respectively. The transcript level was calculated using the FPKM (fragments per kilobase of transcript per million reads) method (Mortazavi et al. 2008). Differential expression analysis between the wild type and *mttpst* was performed using the DESeq. 2 software (Love, Huber, and Anders 2014), and the differentially expressed genes were identified using the following criteria: fold change ≥ 2 and false discovery rate (FDR) < 0.01. Kyoto Encyclopedia of Genes and Genomes (KEGG) pathway analysis was carried out using Python scipy software. The RNA-seq raw data have been deposited in the NCBI Sequence Read Archive under the accession number PRJNA1121021.

2.9 | GUS Histochemical Staining

GUS staining solution was prepared as follows: 100 mM sodium phosphate buffer (pH = 7.0), 10 mM EDTA, 0.5 mM ferricyanide, 0.5 mM ferrocyanide, 0.1% Triton X-100, 20% methanol and 2 mM X-Gluc. *pMtTPST*:*GUS* transgenic roots and nodules were vacuum infiltrated for 10 min and subsequently incubated in the GUS solution at 37°C for 1 h. The samples with GUS signals were observed and photographed under a Stemi 508 stereomicroscope (Carl Zeiss, Jena, Germany).

2.10 | Paraffin-Embedded Sections

M. truncatula nodules (2 wpi) were fixed in FAA (50% ethanol, 5% formaldehyde and 10% acetic acid) solution overnight, dehydrated in a graded ethanol series and embedded in paraffin. The paraffin-embedded samples were sectioned at 5-μm thickness using an RM2235 rotary microtome (Leica, Wetzlar, Germany), stained with 0.05% toluidine blue and examined and photographed under a bright-field microscope (Axio Scope A1, Carl Zeiss, Jena, Germany).

3 | Results

3.1 | Sequence and Phylogeny of TPST Proteins

In a search of genome databases of legume species (phytozome-next.jgi.doe.gov) using the *Arabidopsis* TPST (AtTPST) sequence as a query, putative TPST orthologues were identified in legumes. As

in *Arabidopsis*, all legume species genomes have a single TPST-encoding gene: *MtTPST* (Medtr4g058890) in *M. truncatula*, *LjTPST* (Lj3g0027876) in *L. japonicus*, *GmTPST* (Glyma.11G145300) in *Glycine max*, *PvTPST* (Phvul.011G080300) in *Phaseolus vulgaris* and *VuTPST* (Vigun11g141300) in *Vigna unguiculata*. These TPST proteins have 488-494 amino acids, similar in length to AtTPST, which has 500 amino acids (Komori et al. 2009). Sequence alignment demonstrated that these legume TPST proteins have 86%–94% sequence similarity and share approximately 75% sequence similarity with AtTPST (Figure S1). Additionally, all TPSTs contain a predicted N-terminal signal peptide, a predicted single transmembrane domain near the C-terminus and a conserved C-terminal motif rich in basic amino acids that may function as a subcellular targeting signal (Figure S1) (Komori et al. 2009). Phylogenetic analysis showed that the legume TPSTs cluster into one clade (Figure 1a), suggesting that they are more closely related to each other than to TPSTs from other species (including reported AtTPST and SlTPST and predicted GhTPST, PtTPST, OsTPST and SbTPST) and implying conserved roles of TPSTs in legumes.

3.2 | Expression Patterns of *MtTPST* in *M. truncatula*

To determine expression patterns of *MtTPST* during *M. truncatula* growth and development, qRT-PCR was performed on cDNA derived from various organs (including young nodule, root, stem, leaf, flower, pod and seed) and meristematic tissues (including shoot apical meristem, leaf

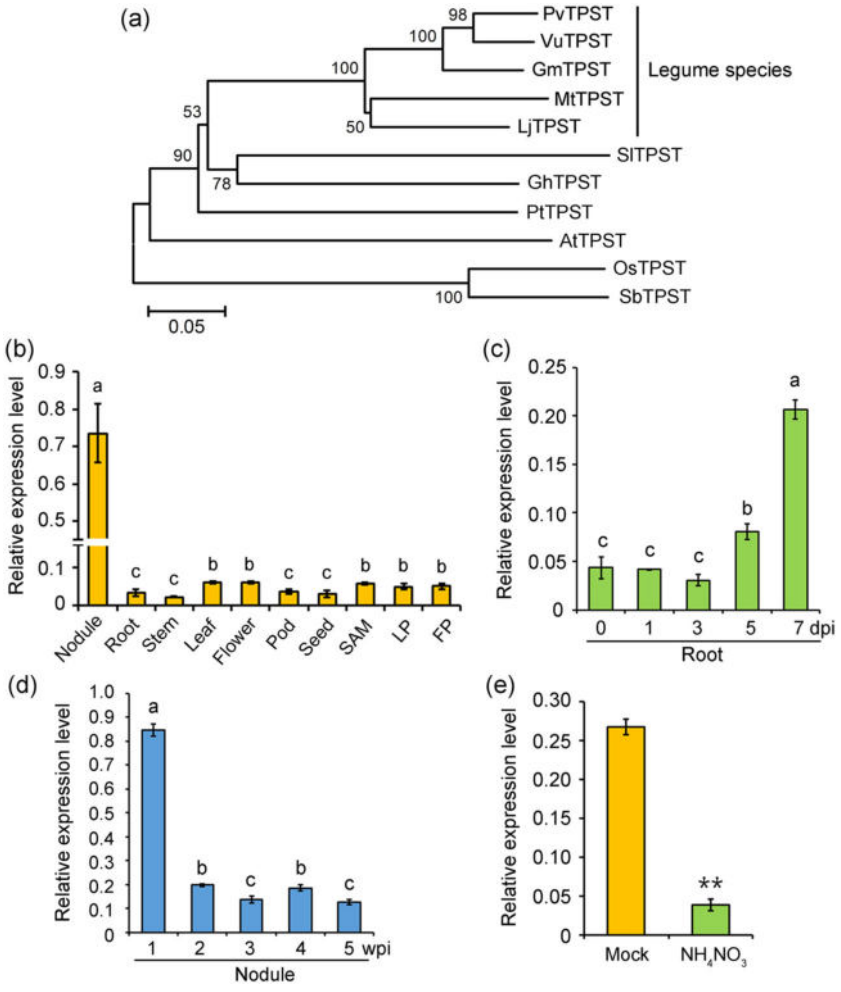

FIGURE 1 | Expression patterns of *MtTPST*. (a) Phylogenetic tree of legume TPST proteins and their orthologues from other plant species. The sequences are from *Phaseolus vulgaris* (PvTPST), *Vigna unguiculata* (VuTPST), *Glycine max* (GmTPST), *Medicago truncatula* (MtTPST), *Lotus japonicus* (LjTPST), *Solanum lycopersicum* (SlTPST), *Gossypium hirsutum* (GhTPST), *Populus trichocarpa* (PtTPST), *Arabidopsis thaliana* (AtTPST), *Oryza sativa* (OsTPST) and *Sorghum bicolor* (SbTPST). The sequences of the TPST proteins used are listed in Table S1. The tree was constructed using MEGA6 software with the neighbour-joining method; bootstrap values from 1000 replications are included. (b) qRT-PCR analysis of *MtTPST* transcript levels in various tissues of *M. truncatula* (A17 ecotype). The tissues examined included root nodules (1-week post-inoculation, 1 wpi), uninoculated roots, stems, leaves, flowers, pods (without seeds), seeds, shoot apical meristems (SAM), leaf primordia (LP) and flower primordia (FP). (c) *MtTPST* transcript abundance measured by qRT-PCR in *M. truncatula* roots inoculated with *Sinorhizobium meliloti* 2011 for 0–7 days. Days post-inoculation, dpi. (d) Expression level of *MtTPST* in *M. truncatula* root nodules at 1–5 wpi. (e) *MtTPST* transcript level detected in *M. truncatula* nodules (3 wpi) treated with or without 10 mM NH_4NO_3 for 4 days. Values are the mean ± SD of three biological replicates normalized against the reference gene *MtActinB*. For (b–d), statistically significant differences indicated by different letters were determined by one-way ANOVA, $p < 0.01$. For (e), asterisks indicate a significant difference determined by Student's *t* test. $^{**}p < 0.01$. [Color figure can be viewed at wileyonlinelibrary.com]

primordium and flower primordium). The results showed that *MtTPST* was expressed in all organs and tissues examined, with much higher transcript level (12- to 34-fold) detected in developing young nodules than in other organs and meristematic tissues (Figure 1b). Analysis of expression pattern from the online *M. truncatula* A17 gene chip data (Benedito et al. 2008) further supported our findings that *MtTPST* was predominantly expressed in developing nodules, with substantial but much lower expression being detected in other organs and meristematic tissues (Figure S2). To investigate the temporal expression pattern during nodule initiation, *MtTPST* expression was examined by qRT-PCR in *M. truncatula* roots inoculated with *S. meliloti* for 0, 1, 3, 5 and 7 days. The results showed that *MtTPST* expression increased at 5 days post-inoculation (dpi) and continued to rise until 7 dpi (Figure 1c), at which stage the young nodules emerged.

During *M. truncatula* nodule development, *MtTPST* expression was detected at all stages, with the highest level detected in nodules at 1 week post-inoculation (wpi) (Figure 1d). Furthermore, *MtTPST* expression in nodules was remarkably repressed after treatment with nitrogen (10 mM NH_4NO_3) (Figure 1e), suggesting possible involvement of *MtTPST* in nodule development.

To investigate the expression pattern of *MtTPST* at the tissue level, a *promoter:GUS* assay was carried out using the *M. truncatula* hairy root transgenic system. The *pMtTPST*:*GUS* plasmid was constructed and transformed into *M. truncatula* hairy roots. Histochemical staining revealed that *pMtTPST*:*GUS* was highly expressed in the root apical meristem (Figure 2a,b), and a high level of GUS activity was observed in lateral root primordia and emerged lateral roots (Figure 2c,d). Furthermore, *pMtTPST*:*GUS* expression was detected throughout nodule developmental processes (Figure 2e–i), consistent with

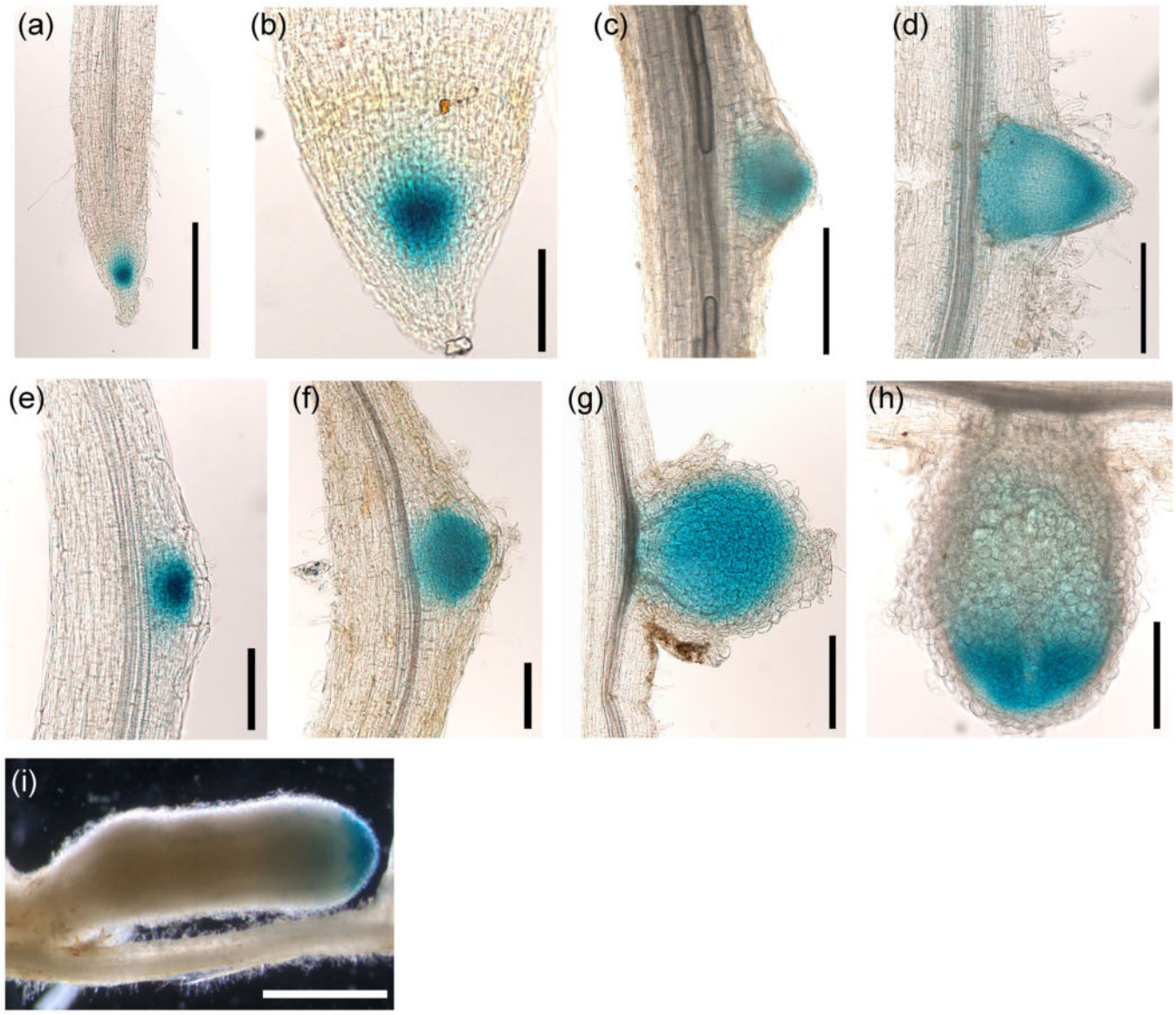

FIGURE 2 | Histochemical staining of *pMtTPST*:*GUS* transgenic hairy roots of *Medicago truncatula*. (a, b) Histochemical GUS staining of roots (a) and root tips (b). (c, d) GUS signals detected in lateral root primordia (c) and emerged lateral roots (d). (e–h) GUS staining of developing nodules at 2 dpi (e), 4 dpi (f), 7 dpi (g) and 14 dpi (h). (i) GUS staining of mature nodules at 21 dpi. Bars = 300 μm in (a, c, d, g and h), 100 μm in (b, e and f) and 1 mm in (i). [Color figure can be viewed at wileyonlinelibrary.com]

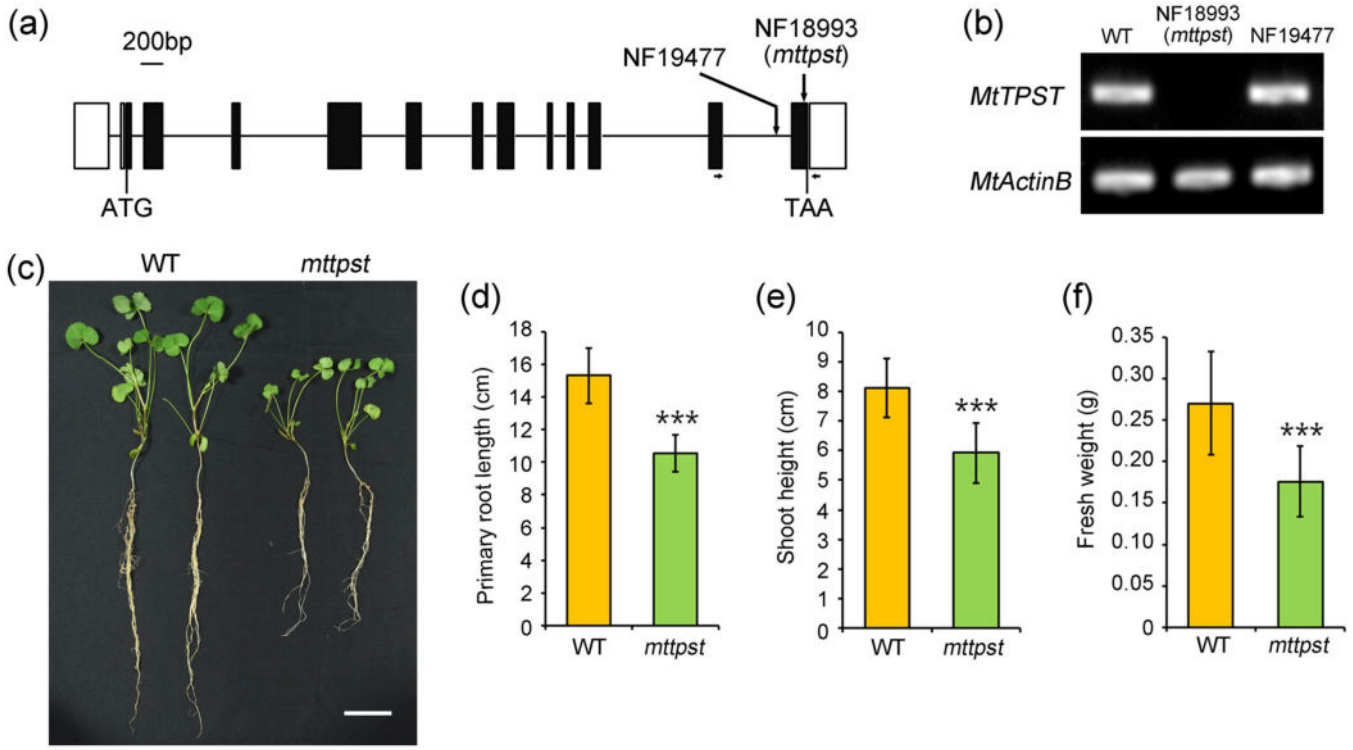

FIGURE 3 | Growth phenotypes of *MtTPST* loss-of-function mutants. (a) Schematic representation of the *MtTPST* gene structure and *Tnt1* insertional sites of mutants. Exons are represented by black boxes, introns by lines and UTRs by white boxes. The NF18993 (*mttpst*) line has a *Tnt1* insertion at the last exon, and the NF19477 line has a *Tnt1* insertion at the last intron. The arrows indicate the positions of primers used for identification of *MtTPST* mutants. (b) Semiquantitative RT-PCR analysis of *MtTPST* transcript levels in wild-type *Medicago truncatula* (R108) and mutant lines. Expression of *MtActinB* was used as an internal control. (c) Comparison of wild-type (R108) and *mttpst* mutant plants at 21 days post-inoculation (dpi) with *Sinorhizobium meliloti* 2011. Bar = 3 cm. (d–f) Measurements of primary root length (d), shoot height (e) and fresh weight (f) of wild-type and *mttpst* plants at 21 dpi. Values are the mean ± SD from $n = 30$ (WT) and 25 (*mttpst*) plants. Statistical significance was determined by Student's *t* test. ***$p < 0.001$. Experiments were repeated three times, with similar results. [Color figure can be viewed at wileyonlinelibrary.com]

the qRT-PCR expression pattern (Figure 1d). Specifically, at 2 dpi, an intense GUS signal was detected in the cortical cells of the root's susceptible zone, corresponding to the incipient nodule primordium (Figure 2e). With the development of the nodule primordium, *pMtTPST*:*GUS* was persistently expressed at a high level in the whole primordium (Figure 2f). At 7 dpi, the primordium emerged as a young nodule, in which GUS signals occupied the entire central tissues (Figure 2g). However, from 7 dpi, GUS staining faded gradually from the base of the nodule. At 14 dpi, and especially at 21 dpi, the GUS signal was restricted to the nodule apical region, corresponding mainly to meristematic and infection zones (Figure 2h,i). These results indicate that MtTPST might be involved in nodule initiation and development as well as in root growth.

3.3 | Growth Phenotypes of a Loss-of-Function Mutant of *MtTPST*

To investigate the biological function of *MtTPST*, two homozygous *Tnt1*-insertion mutants (NF18993 and NF19477) of this gene were identified from the Nobel Foundation *M. truncatula* mutant library. NF18993 and NF19477 harbour a *Tnt1* insertion in the last exon and the last intron of the *MtTPST* gene, respectively (Figure 3a). A semiquantitative RT-PCR assay demonstrated that *MtTPST* expression was abolished only in NF18993 (Figure 3b), which is referred to as *mttpst* hereafter. Growth phenotypical observation at 3 wpi with *S. meliloti* 2011 revealed that *mttpst* plants had obviously stunted shoots and roots (Figure 3c). Based on statistical analyses, primary root length and shoot height in *mttpst* were decreased by 31% and 27%, respectively (Figure 3d,e), compared with wild type, and both the lateral root number per plant and lateral root density were significantly reduced (Figure S3a-c). Accordingly, plant fresh weight was reduced by 35% in *mttpst* plants (Figure 3f). Furthermore, *mttpst* developed smaller leaves and fruits (Figure S3d), and mature seeds in *mttpst* also exhibited smaller sizes (Figure S3e), with the one-hundred seed weight decreasing by 22% compared with that of wild type (Figure S3f).

3.4 | Symbiotic Phenotypes of the *Mttpst* Mutant

Given that *MtTPST* is highly expressed in root nodules, we evaluated the symbiotic nodulation phenotypes of the *mttpst* mutant. At 3 wpi with *S. meliloti*, *mttpst* produced obviously fewer nodules than wild-type plants (Figure 4a). Counting the nodules per plant revealed that both pink (mature) and white (immature) nodules on *mttpst* plants were significantly reduced compared with those on wild-type plants, with the total nodule (pink plus white) number decreasing by 63% (Figure 4b). Furthermore, to differentiate the effect of root length on nodule number, we calculated the nodule density based on the unit length of primary roots. The results showed that the nodule

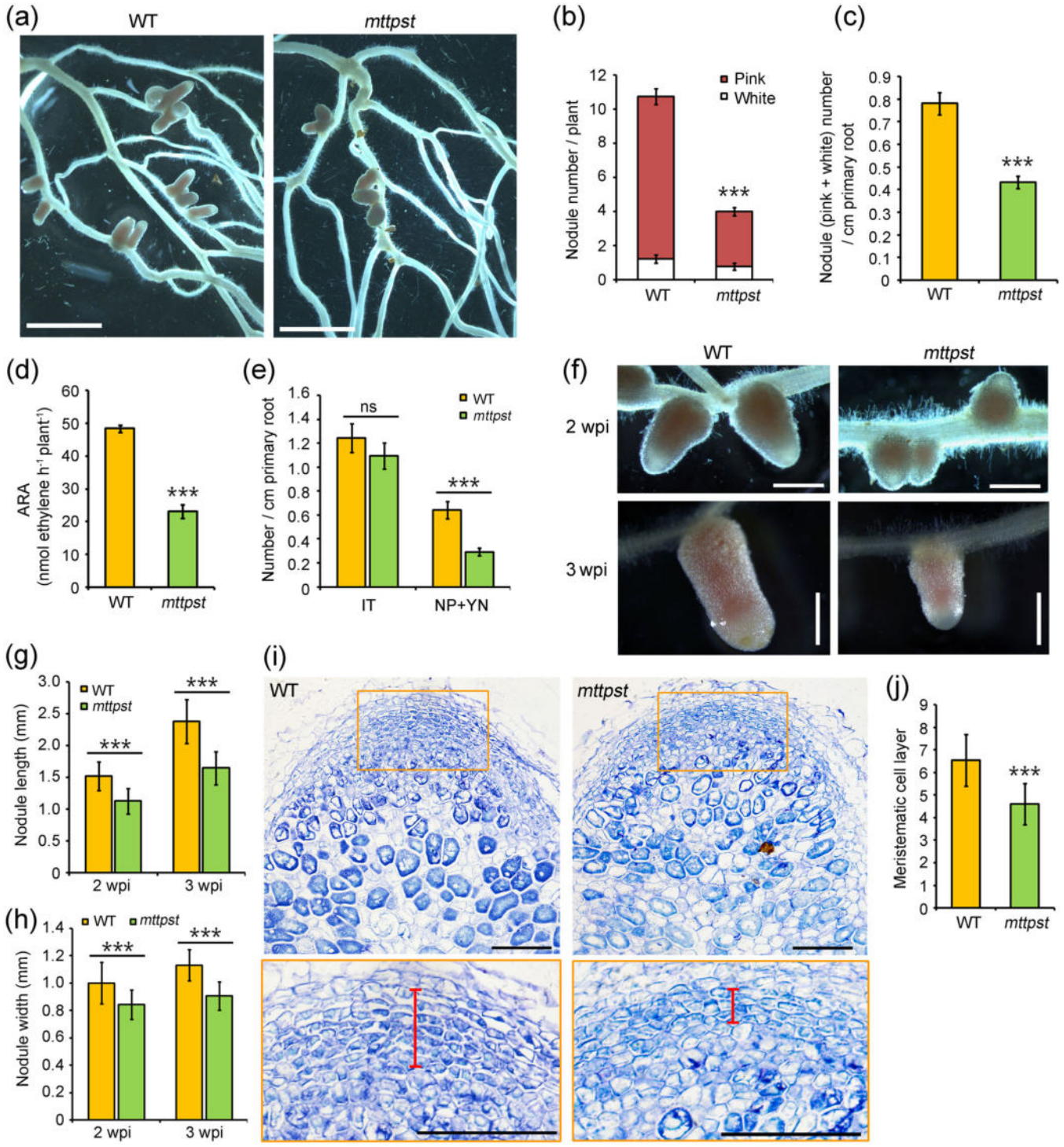

FIGURE 4 | Symbiotic phenotypes of the *mttpst* mutant. (a) Nodulation phenotype of wild type (R108) and *mttpst* at 3 weeks post-inoculation (wpi) with *Sinorhizobium meliloti* 2011. Bars = 5 mm. (b) Number of nodules formed on wild-type and *mttpst* roots at 3 wpi. (c) Nodule (including pink and white) numbers per unit length (cm) of the primary root at 3 wpi. Data in (b, c) are the mean ± SE from $n = 18$ plants. (d) Nitrogenase activities of wild-type and *mttpst* nodules per plant. (e) Numbers of infection threads (ITs) and nodule primordia (NPs) (including emerged young nodules [YNs]) of wild-type and *mttpst* plants at 7 dpi. Data are the mean ± SE from $n = 23$ (WT) and 32 (*mttpst*) plants. (f) Nodules of wild type and *mttpst* at 2 and 3 wpi. Bars = 1 mm. (g, h) Length (g) and width (h) of wild-type and *mttpst* nodules at 2 and 3 wpi. Data are the mean ± SD from 47 to 70 nodules. (i) Longitudinal sections of nodules at 2 wpi. The lower pictures are the close-up of the boxed area of the upper pictures. Red bars indicate meristematic zones at the nodule tips. Bars = 100 μm. (j) Numbers of meristematic cell layers of wild-type and *mttpst* nodules. Data represent the mean ± SD, $n = 18$. In (b–e, g, h, j), statistical significance was determined by Student's *t* test. ***$p < 0.001$; ns, not significant. Experiments were repeated three times, with similar results. [Color figure can be viewed at wileyonlinelibrary.com]

number per centimetre of the primary root of the *mttpst* plants was decreased by 44% compared with that of wild type (Figure 4c). Furthermore, an acetylene reduction assay revealed significantly reduced nitrogenase activities in *mttpst* plants (Figure 4d). It is known that root nodule formation is originally determined by rhizobial infection and nodule initiation, and we thus examined the effect of *MtTPST* loss-of-function mutant on these two processes. As depicted in Figure 4e, IT formation was not significantly affected in *mttpst*; however, the number of nodule primordia (including young nodules) per unit root length was decreased remarkably in *mttpst* compared to wild type. These findings, combined with the expression pattern (Figure 2e,f), indicate that *MtTPST* positively regulates nodulation by enhancing nodule initiation and primordium formation.

Given that *MtTPST* is primarily expressed in the apical meristem of nodules at 2–3 wpi (Figure 2h,i), we observed nodule growth phenotypes. As illustrated in Figure 4f, the nodules formed on *mttpst* plants were obviously smaller than those on wild-type plants, with the length of *mttpst* nodules decreasing by 26%–31% at 2 and 3 wpi (Figure 4g), and the width decreasing by 16%–20% (Figure 4h). To investigate the effect of MtTPST on nodule growth at the cellular level, longitudinal sectioning of nodules at 2 wpi was performed. The *mttpst* nodules had smaller meristem zones, with the layer number of meristematic cells decreasing by 30% in *mttpst* nodules compared with wild type (Figure 4i,j). These results suggest that MtTPST promotes nodule growth by regulating the proliferation of meristematic cells.

3.5 | *MtTPST* Complemented the Phenotypes of *mttpst* and the *Arabidopsis tpst-1* Mutant

To investigate whether the *mttpst* mutant is dominant or recessive, we back-crossed *mttpst* with wild-type (R108) plants, and the resulting F1 generation was self-fertilized to generate an F2 population. The F2 individuals segregated in a 3:1 ratio of wild type to mutant phenotypes (58 wild-type-like plants, 19 mutant plants with defective growth and symbiotic phenotypes, $\chi^2 = 0.004$, $p > 0.05$), indicative of a monogenic-recessive mutant. Furthermore, PCR-based genotyping of the back-crossed F2 population revealed that the *mttpst* genotype cosegregated perfectly with the mutant phenotype (Figure S4).

To confirm that the pleiotropic phenotypes of the *mttpst* mutant are caused by the absence of MtTPST function, we constructed the *pMtTPST:MtTPST* complementary expression plasmid and transformed it into *mttpst* via *Agrobacterium tumefaciens*. qRT-PCR assays revealed that the complemented transgenic lines had a *MtTPST* transcript level similar to that of wild type (Figure 5a). Moreover, phenotypic observation revealed that growth and development were rescued in the *pMtTPST:MtTPST*-complemented plants (Figure 5b), with symbiotic and growth parameters, such as nodule number, primary root length, shoot height and fresh weight, being comparable to those of wild type (Figure 5c–f). These results indicate that loss of function of *MtTPST* is responsible for the observed defective phenotypes of the *mttpst* mutant.

Given that MtTPST shares high sequence similarity with AtTPST at the protein level, it is reasonable to presume that TPST function is conserved between *M. truncatula* and *Arabidopsis*. To test this assumption, we constructed the *pAtTPST:MtTPST* plasmid, in which *MtTPST* expression is controlled by the *AtTPST* promoter, and transformed it into the *AtTPST* loss-of-function mutant *tpst-1*. As shown in Figure 5g, *tpst-1* seedlings exhibited markedly shortened roots, which is consistent with a previous report (Komori et al. 2009), whereas the *pAtTPST:MtTPST*-complemented seedlings developed normal roots, with lengths indistinguishable from those of wild type (Figure 5g,h). In addition, when grown in soil for 4 weeks, heterogeneous expression of *MtTPST* fully rescued the defective growth phenotype of *tpst-1* (Figure S5a), with leaf size and plant weight comparable to those of wild type (Figure S5b–d). These findings suggest that MtTPST and AtTPST are orthologues conserved during evolution.

3.6 | Overexpression of *MtTPST* Increased Nodule Number

To further investigate the biological functions of MtTPST, we constructed a constitutive overexpression plasmid under control of the enhanced cauliflower mosaic virus (CaMV) 35S promoter and transformed the resulting *35S:MtTPST* construct into *M. truncatula* hairy roots mediated by *Agrobacterium rhizogenes*. qRT-PCR assays revealed that *MtTPST* was successfully overexpressed in the transgenic hairy roots (Figure 6a). At 3 wpi with *S. meliloti*, the *MtTPST*-overexpressing lines produced obviously more nodules (Figure 6b,c), with the nodule number per plant increasing by 51% compared with control plants (Figure 6d). Moreover, hairy root length was also promoted by *MtTPST*-overexpression (Figure 6e). To differentiate the effect of root length on nodule number, we calculated the nodule frequency based on the unit length of hairy roots. The results showed that the nodule density of the overexpression plants was increased by 34% compared with control plants (Figure 6f). Furthermore, the early symbiotic events investigation revealed that *MtTPST*-overexpression significantly increased the number of nodule primordia (including young nodules) per unit root length, while the IT formation was not affected (Figure 6g). However, unexpectedly, the nodule length was not significantly altered by *MtTPST* overexpression (Figure 6h). These findings indicate that *MtTPST* positively regulates nodulation by enhancing nodule initiation.

To investigate whether MtTPST's function on nodulation depends on the Nod factor signalling, we transformed the *35S:MtTPST* construct into the hairy roots of *nfp* and *nin* mutants which were defective in Nod factor signalling. The results showed that *MtTPST*-overexpression did not induce nodulation of these two nodule-deletion mutants (Figure S6). These findings indicate that overproduced MtTPST promotes nodulation in a Nod factor signalling-dependent manner.

3.7 | PSK and RGF3 Peptides Partially Rescued the Phenotypes of *mttpst*

In *Arabidopsis*, AtTPST catalyses tyrosine sulfation of several classes of peptides to achieve their full activities, and treatment

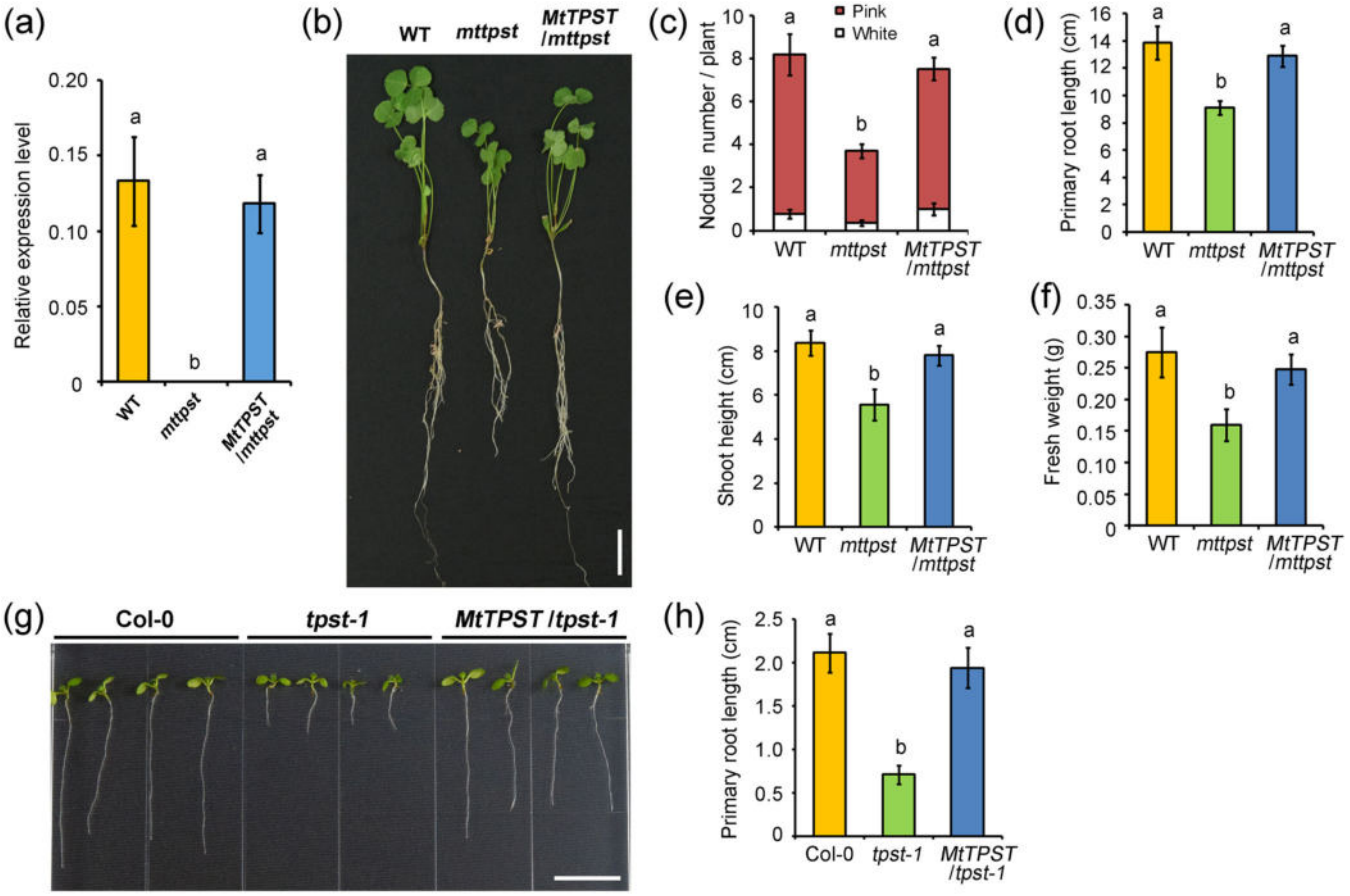

FIGURE 5 | Genetic transformation of the *MtTPST* gene complemented the phenotypes of *mttpst* and *Arabidopsis tpst-1*. (a) qRT-PCR analysis of *MtTPST* expression levels in wild type (R108), *mttpst*, and *pMtTPST:MtTPST* transgenic lines in the *mttpst* background (*MtTPST/mttpst*). Values are the mean ± SD of three biological replicates normalized against the reference gene *MtActinB*. (b) Phenotypes of wild type, *mttpst* and *MtTPST/mttpst* at 3 wpi with *Sinorhizobium meliloti* 2011. Bar = 2 cm. (c–f) Nodule numbers per plant (c), primary root length (d), shoot height (e) and fresh weight (f) of the indicated genotypes of *Medicago truncatula* at 3 wpi. (g) Six-day-old *Arabidopsis* seedlings of wild type (Col-0), *tpst-1* mutant and *pAtTPST:MtTPST* transgenic line in the *tpst-1* background (*MtTPST/tpst-1*). Bar = 1 cm. (h) Root length of the *Arabidopsis* seedlings shown in (g). $n = 22–30$. Data represent the mean ± SD. Statistically significant differences indicated by different letters were determined with one-way ANOVA ($p < 0.01$). Experiments were repeated three times, with similar results. [Color figure can be viewed at wileyonlinelibrary.com]

with the corresponding sulfated peptide(s) usually rescues the defective phenotypes of the *tpst-1* mutant (Matsuzaki et al. 2010; Igarashi, Tsuda, and Katagiri 2012; Doblas et al. 2017; Ogawa-Ohnishi et al. 2022). Based on the findings that MtTPST shares high sequence similarity with AtTPST (Figure S1) and is a functional orthologue (Figure 5g,h), it is conceivable that MtTPST also functions in posttranslational modification of substrate peptides. In our previous studies, PSK and RGF3 peptides, which are putatively tyrosine-sulfated by TPST, were found to regulate root growth and nodule formation in legume species (Wang, Yu, et al. 2015; Li et al. 2020; Di et al. 2022; Yu et al. 2022). Additionally, PSK peptides, including PSK-α, PSK-δ and PSK-ε, were all able to promote *M. truncatula* root elongation, with PSK-α exhibiting the greatest promotion effect (Figure S7).

To investigate which sulfated peptide(s) are responsible for the *mttpst* phenotypes, we treated 8-day-old mutant seedlings in soil with 1 μM sulfated PSK-α and/or RGF3 peptides with the desulfated peptides as control. The results showed that application of sulfated PSK-α or RGF3 significantly promoted root elongation in *mttpst* and that treatment with both peptides had an additive promotion effect, while the desulfated peptides treatment almost had no activity on root growth promotion (Figure 7a,b), indicating that these two peptides function synergistically in inducing root growth and the tyrosine sulfation mediated by MtTPST is critical for their biological activity. Likewise, treatment of both sulfated PSK-α and RGF3 peptides exhibited an additive effect on promoting *Arabidopsis tpst-1* root elongation (Figure S8), suggesting a conserved function of these two types of sulfated peptides in regulation of root growth. However, we noticed that even in the presence of both PSK-α and RGF3 peptides, the length of the *mttpst* roots could not be recovered to the wild-type level (Figure 7a,b). Given that 1 μM is a relatively high concentration for peptide hormone signalling, this phenomenon might be caused by the possible insufficient absorbance of peptides in the soil environment. If that's really the case that both PSK-α and RGF3 peptides are unable to fully recover root growth, an alternative possibility is that other sulfated peptide(s) are also involved in this process. Moreover, in the symbiotic condition, treatment with sulfated PSK-δ peptide, which exhibits specific high expression in nodules (Yu et al. 2022), partially complemented the symbiotic phenotype with respect to nodule number. In

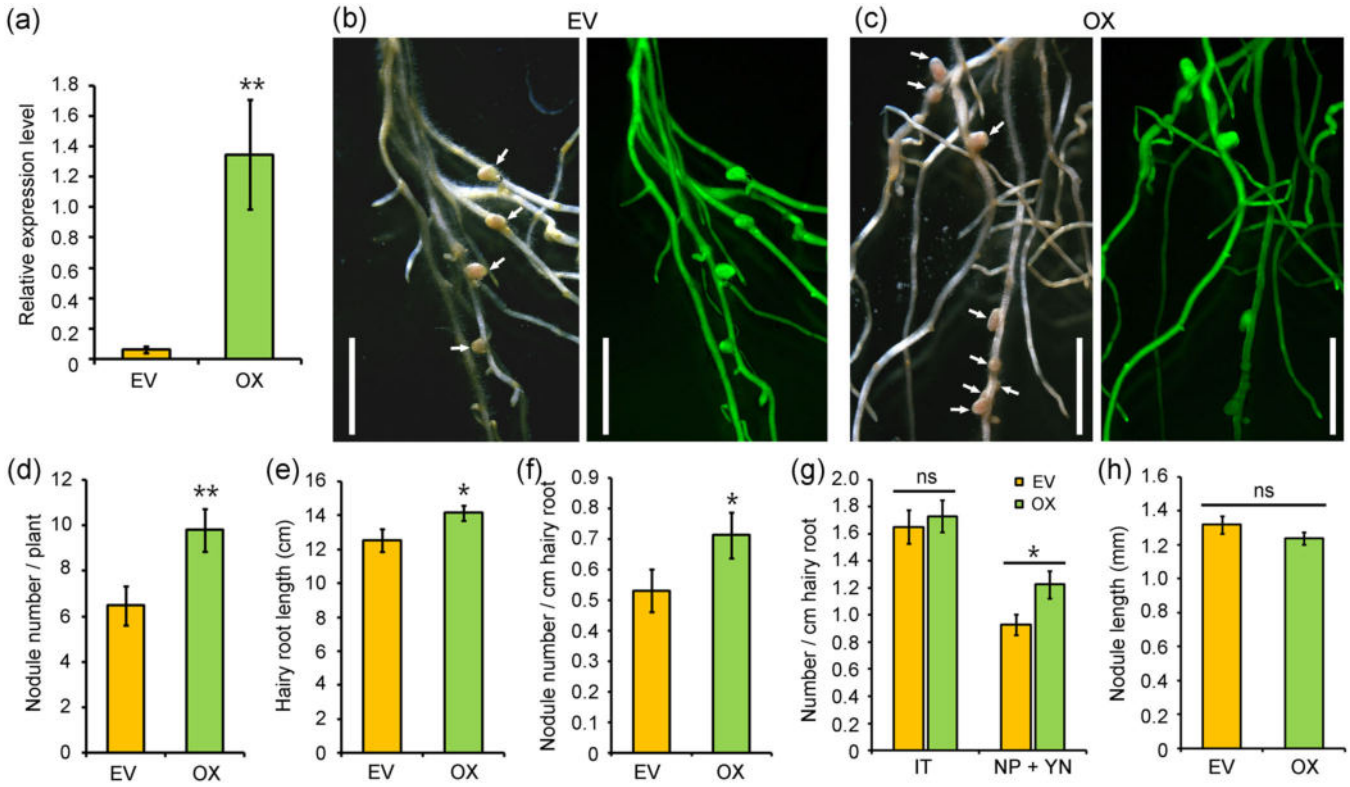

FIGURE 6 | Overexpression of *MtTPST* promoted nodulation in *Medicago truncatula*. (a) qRT-PCR analysis of *MtTPST* transcript levels in *MtTPST*-overexpressing (OX) and empty vector (EV)-transformed *M. truncatula* (A17) hairy roots. Values are the mean ± SD of three biological replicates normalized against the reference gene *MtActinB*. (b, c) Nodulation phenotype of EV (b) and OX (c) transgenic *M. truncatula* roots at 21 dpi. Left panels, bright-field images; right panels, GFP images. Arrows indicate nodules. Bars = 5 mm. (d, e) Nodule number per plant (d) and hairy root length (e) of EV and OX transgenic roots at 21 dpi. (f) Nodule numbers per unit length (cm) of the hairy roots. (g) Numbers of infection threads (ITs) and nodule primordia (NPs) (including emerged young nodules [YNs]) of EV and OX transgenic roots at 7 dpi. (h) Length of nodules formed on the EV and OX transgenic roots. Values are the mean ± SE. $n = 21$. Statistical significance was evaluated by Student's *t* test. $^{*}p < 0.05$, $^{**}p < 0.01$, ns, not significant. Experiments were repeated three times with similar results. [Color figure can be viewed at wileyonlinelibrary.com]

contrast, sulfated RGF3 failed to rescue nodule formation in *mttpst* (Figure 7c). Additionally, treatment with sulfated RGF3 partially rescued the small-nodule phenotype observed at 21 dpi, though application of sulfated PSK-δ had no effect on nodule growth (Figure 7d,e). These results indicate that PSK functions mainly in nodule initiation and primordium formation at the early stage of nodulation, which eventually affects the nodule number; while RGF3 is primarily responsible for nodule growth and maturation at the later stage of nodulation.

3.8 | MtTPST Functions Downstream of the Nod Factor Signalling Pathway

To determine whether Nod factor signalling is required for *S. meliloti*-induced expression of *MtTPST*, we measured its expression level by qRT-PCR in 5 dpi roots of wild-type *M. truncatula* and four Nod factor signalling mutants, including *nfp*, *dmi3*, *nsp1* and *nin*. The results showed that *MtTPST*'s transcript level was remarkably upregulated in wild-type roots compared with that in the uninoculated control. However, the induction effect on *MtTPST* expression was abolished in the mutants (Figure 8a), demonstrating that Nod factor signalling is necessary for induction of *MtTPST* expression. These findings suggest that MtTPST functions downstream of the Nod factor signalling pathway in promoting nodule formation.

3.9 | MtTPST Promotes Nodule Formation Through Regulating Accumulation and/or Signalling of Cytokinin and Auxin

To obtain insights into the molecular mechanism of MtTPST-regulated nodule formation, we conducted an RNA-sequencing analysis on the *S. meliloti*-inoculated roots of wild-type *M. truncatula* and *mttpst* mutant. Sequencing analysis showed that 1178 genes were differentially expressed (fold change ≥ 2, FDR < 0.01) between *mttpst* and wild type, among which 632 genes were downregulated (Table S4) in *mttpst* and 546 genes were upregulated (Table S5). KEGG analysis was performed on the differentially expressed genes (DEGs). As shown in Figure 8b, DEGs involved in 'zeatin (cytokinin) biosynthesis', 'plant hormone signal transduction', 'MAPK (mitogen-activated protein kinase) signalling pathway' and other metabolism pathways were significantly enriched.

Cytokinin is a critical phytohormone positively regulating cortical cell division during nodule organogenesis (Yang et al. 2022). Among the DEGs, *Medtr3g113710*, encoding a putative cytokinin-activating

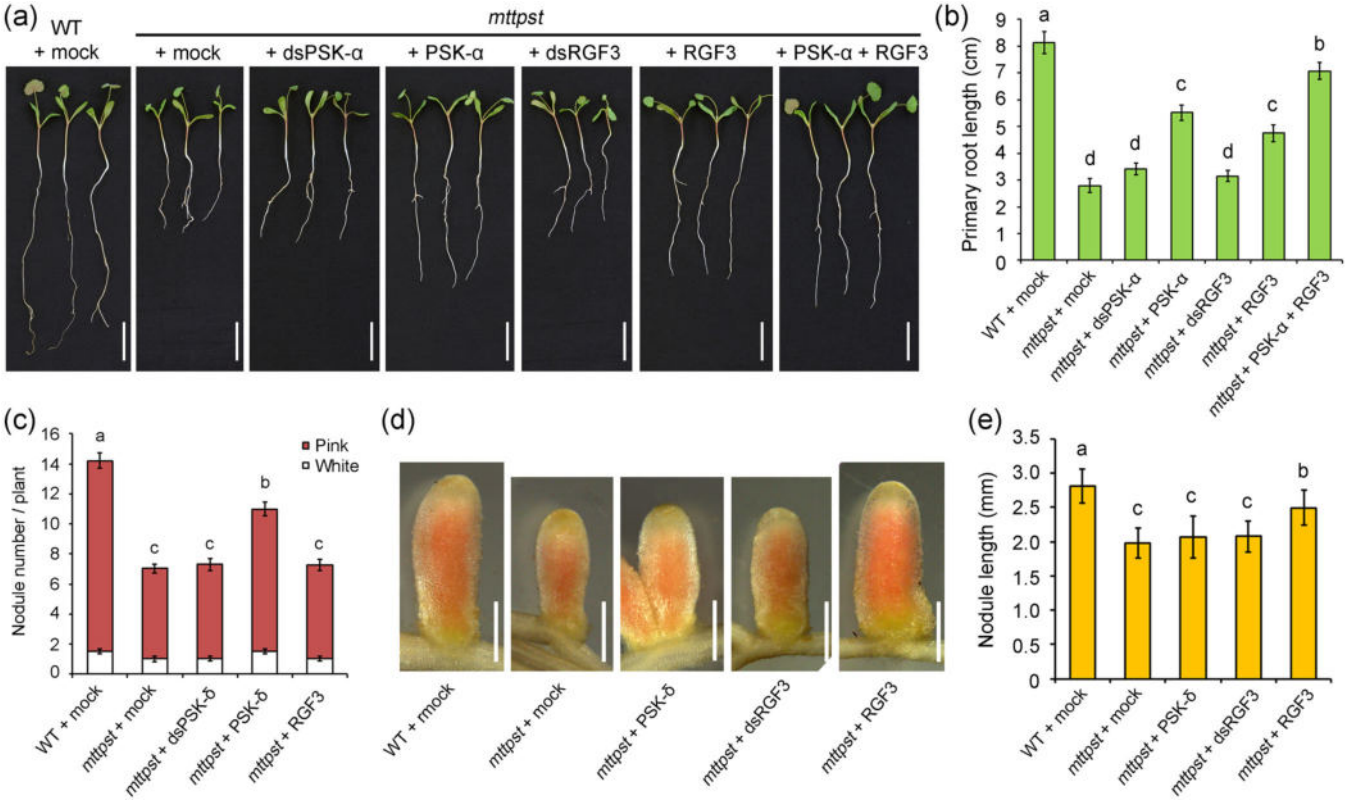

FIGURE 7 | Peptide treatment partially restored the phenotypes of *mttpst*. (a) Germinated seeds of wild type (R108) and *mttpst* were cultured for 8 days with treatment of corresponding peptides (1 μM) in soil. Pictures from left to right are wild-type *Medicago truncatula* treated with water (mock), *mttpst* with water (mock), *mttpst* with desulfated (ds) PSK-α, *mttpst* with PSK-α, *mttpst* with dsRGF3, *mttpst* with RGF3 and *mttpst* with both PSK-α and RGF3. Bars = 2 cm. (b) Primary root length of 8-day-old *M. truncatula* seedlings with each treatment shown in (a). Values are means ± SEs. $n = 18–21$. (c) Nodule number per plant of 21 dpi wild-type and *mttpst* plants treated with the indicated peptides (1 μM). Values are means ± SEs. $n = 28–34$. (d) Representative nitrogen-fixing nodules of wild-type and *mttpst* plants (21 dpi) treated with the indicated peptides (1 μM). Bars = 1 mm. (e) Statistical analysis of the length of nodules shown in (d). Values are means ± SDs. $n = 32–34$. In (b, c, e), statistically significant differences indicated by different letters were determined with one-way ANOVA ($p < 0.01$). [Color figure can be viewed at wileyonlinelibrary.com]

enzyme LONELY GUY (LOG), was transcriptionally down-regulated in *mttpst* compared to the wild type, while the putative degradation enzyme cytokinin oxidase/dehydrogenase (CKX)-encoding gene *Medtr7g090920* was significantly upregulated (Figure 8c and Tables S4 and S5), indicating that MtTPST promotes cytokinin accumulation during nodule formation. In the 'plant hormone signal transduction' term, a gene (*Medtr2g100520*) encoding for a putative IAA-amino acid hydrolase ILR1 was repressed in *mttpst*, and several auxin-responsive genes with possible roles involved in auxin signalling were also transcriptionally down-regulated in *mttpst*, including three SAUR (small auxin up RNA) genes (*Medtr1g063330*, *Medtr8g096440* and *Medtr8g096500*), one ARF (auxin-responsive factors) gene (*Medtr1g076270*) and three DRM1/ARP (dormancy/auxin associated protein) genes (*Medtr1g083440*, *Medtr2g014240* and *Medtr8g022300*) (Figure 8c and Table S4). These results are consistent with the importance of auxin signalling during nodule organogenesis (Liu et al. 2018). In addition, several MAPKKK (MAPK kinase kinase)-encoding genes (*Medtr2g088020*, *Medtr5g071560* and *Medtr0189s0010*) had lower expression levels in *mttpst* than in wild type (Figure 8c and Table S4), suggesting that MtTPST might regulate nodulation through influencing the MAPK signalling pathway.

Peptide treatment and phenotypic analysis have revealed that the sulfated PSK-δ peptide partially recovered the defective nodulation capacity of *mttpst* (Figure 7c). To further investigate the molecular mechanism of MtTPST-PSK-δ module in regulation of nodule formation, we treated *mttpst* seedlings with 1 μM PSK-δ for 24 h in the symbiotic condition. Roots of the PSK-δ-treated *mttpst* and of the mock-treated wild-type and *mttpst* seedlings were collected for qRT-PCR analysis of the expression of the above cytokinin/auxin/MAPKKK-associated DEGs. Consistent with the RNA-seq data, the qRT-PCR results showed that these genes were transcriptionally down- or upregulated in *mttpst* relative to the wild type, and application of the PSK-δ peptide to *mttpst* restored gene expression to or near wild-type levels, with the exception of *Medtr5g071560* (Figure 8d–f). Together, combined analyses of RNA-seq and qRT-PCR results demonstrate that MtTPST, mainly through sulfated PSK-δ, promotes nodule formation via regulating accumulation and/or signalling of cytokinin and auxin.

It is known that the root meristematic marker genes, such as *PLETHORAs* (*PLTs*) and *WUSCHEL-RELATED HOMEOBOX 5* (*WOX5*), also have a specific expression in legume nodule primordium and meristem (Franssen et al. 2015; Osipova et al. 2012), consistent with the expression pattern of *MtTPST* in nodule formation. To investigate the regulatory relationship of *MtTPST* and these marker genes, we searched the RNA-seq data and found that the transcript level of *MtPLTs* and *MtWOX5* was not significantly altered in inoculated roots

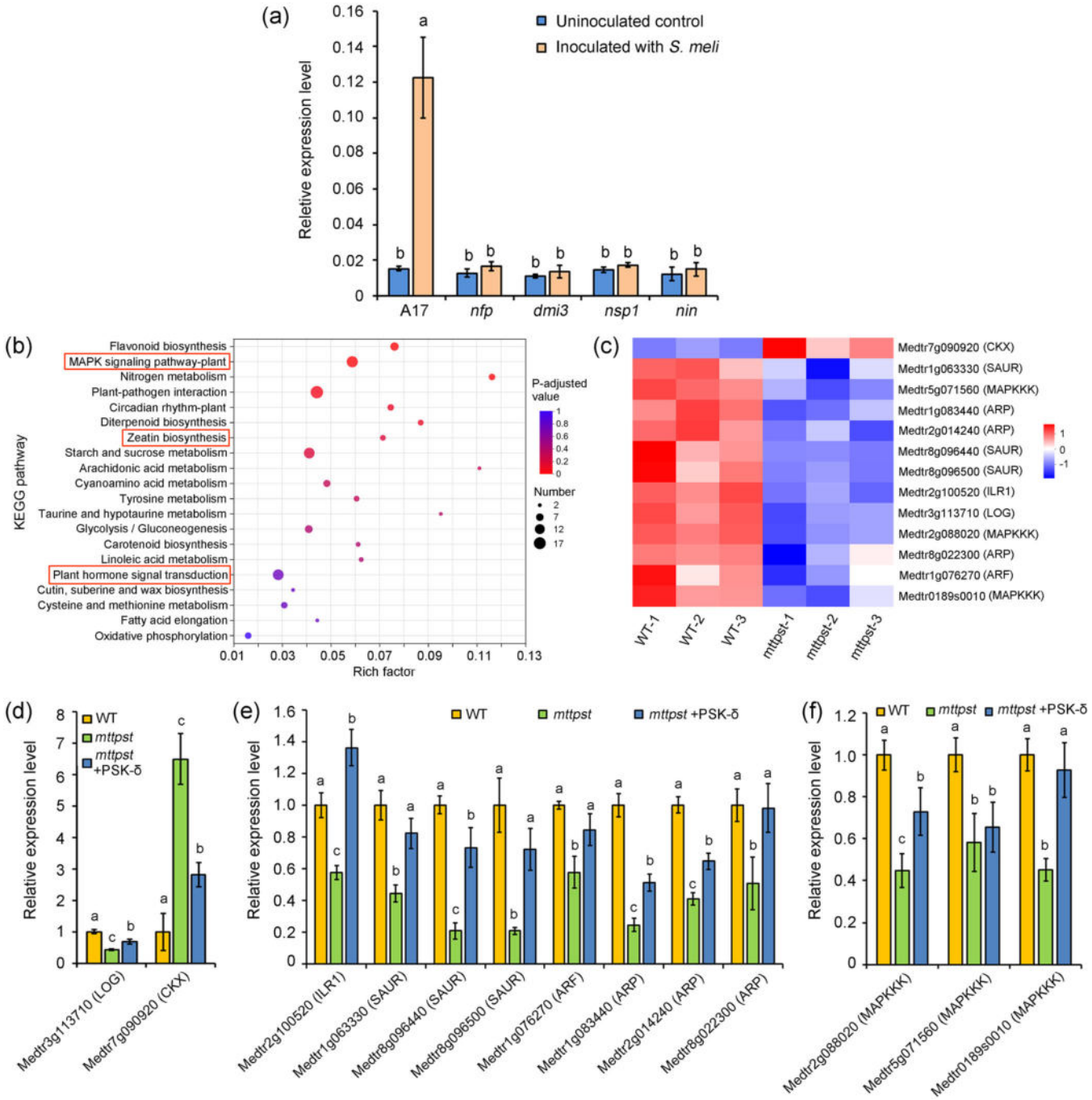

FIGURE 8 | MtTPST functions downstream of the Nod factor signalling and transcriptome analysis of downstream genes of *MtTPST*. (a) Expression analysis of *MtTPST* by qRT-PCR in roots of wild-type *Medicago truncatula* (A17) and four symbiotic nodulation mutants at 5 dpi, with expression in uninoculated roots at 5 days as controls. (b) KEGG pathway analysis of DEGs between *mttpst* and wild type. (c) Heat map showing the expression alteration of cytokinin/auxin/MAPKKK-associated DEGs between *mttpst* and wild type. (d–f) qRT-PCR analyses of the expression levels of cytokinin (d)/auxin (e)/MAPKKK (f) -associated genes in roots of mock-treated wild-type and *mttpst* and PSK-δ-treated *mttpst* seedlings in the symbiotic condition. [Color figure can be viewed at wileyonlinelibrary.com]

of *mttpst* compared to the wild type. Considering that *MtPLT3/4* (Franssen et al. 2015) and *MtWOX5* (Osipova et al. 2012) have an overlapping expression with *MtTPST* in the meristem zones of developing nodules, we examined their expression levels in 2 wpi nodules of wild-type *M. truncatula* and *mttpst* by qRT-PCR assays. As shown in Figure S9, none of these genes was transcriptionally influenced by *MtTPST* mutation. These results indicate that MtTPST-mediated sulfated peptide signalling does not affect these meristematic marker genes at the transcript level during nodule formation. It is worth noting that, in *Arabidopsis*, TPST-RGF module regulates the maintenance of root stem cells by defining PLT levels at the posttranscriptional level (Matsuzaki et al. 2010) and enhancing PLT protein stability at the posttranslational level (Yamada, Han, and Benfey 2020). Therefore, although MtTPST does not affect the transcript levels of *MtPLTs* during nodule formation, it may regulate their abundance at the posttranscriptional or posttranslational levels.

4 | Discussion

4.1 | *MtTPST* Is a Conserved Gene Responsible for Peptide Sulfation Involved in Nodule Formation and Root Growth

AtTPST is the single-copy TPST-encoding gene in *Arabidopsis* and is responsible for posttranslational modification of all functional sulfated peptide hormones (Komori et al. 2009). Intriguingly, in tomato (*Solanum lycopersicum*), TPST is also encoded by a single-copy gene, *SlTPST* (Zhang et al. 2018). In addition, the predicted *TPSTs* in several plant species, including *Populus trichocarpa*, *Oryza sativa* and *Sorghum bicolor*, are all single-copy genes (Zhou et al. 2010). Through sequence alignment in legume genome databases, we identified a single *TPST* gene from each legume species. These legume TPSTs have high sequence similarities with AtTPST. These findings strongly indicate that *TPSTs* are evolutionarily conserved genes in the plant kingdom. The loss-of-function mutant of *MtTPST* displayed similar defective phenotypes, including dwarf shoots and short roots, as the *Arabidopsis tpst-1* mutant, and heterogeneous expression of *MtTPST* fully complemented the defective phenotypes of *tpst-1*, indicating that MtTPST is a functional orthologue of AtTPST involved in controlling peptide sulfation.

The phylogenetic tree shows that the legume TPSTs have a closer phylogenetic relationship relative to other members and cluster into a legume-specific clade, indicating that these TPSTs might be involved in legume-specific developmental processes, such as symbiotic nodulation. Indeed, functional dissection revealed that MtTPST controls not only nodule number but also nodule growth in *M. truncatula* partially by regulating PSK and RGF3 peptide maturation.

4.2 | MtTPST Is a Key Regulator of Root Growth via Sulfated PSK and RGF3 Peptides

The *promoter:GUS* assay showed that *MtTPST* was highly and specifically expressed in the root apical meristem of *M. truncatula* primary roots, consistent with *AtTPST*'s expression in *Arabidopsis* roots (Komori et al. 2009; Zhou et al. 2010). The loss-of-function mutant *mttpst* displayed a short-root phenotype similar to the *Arabidopsis tpst-1* mutant. These *tpst-1* roots exhibited decreased meristematic activity caused by deficiency of sulfated RGF peptides and reduced cell elongation activity due to loss of sulfated PSK and PSY1 peptides. Consistently, simultaneous application of RGF, PSK and PSY1 peptides successfully restored the root growth phenotype of *tpst-1* (Matsuzaki et al. 2010). Based on the findings that both the *MtPSKδ* and *MtRGF3* genes are intensively expressed in *M. truncatula* root tips, including the meristematic and partial elongation zones (Li et al. 2020; Yu et al. 2022), and that the three PSK members (PSK-α, PSK-δ and PSK-ε) have promotive effects on root elongation, with PSK-α having the highest expression, we treated *mttpst* seedlings with synthetic PSK-α and RGF3 peptides, representing the PSK and RGF families, respectively. As expected, application of each sulfated peptide, but not the unsulfated counterpart, partially restored root length and treatment with both sulfated peptides showed an additive effect but still did not fully recover the root phenotype. These results suggest that MtTPST-mediated tyrosine-sulfation of PSK, RGF and other peptide(s) is needed for root elongation induction (Figure 9).

pMtTPST:GUS activities were also detected in *M. truncatula* lateral root primordia and emerged lateral roots, which is reminiscent of a similar expression pattern of *AtTPST* in lateral root formation (Komori et al. 2009). Although PSKs and RGFs act synergistically in promoting root elongation (Kutschmar et al. 2009; Matsuzaki et al. 2010; Fernandez et al. 2013; Yu et al. 2016), their roles in lateral root formation seem to be opposite. For instance, PSK-ε peptide treatment and overexpression of its precursor gene both increased lateral root density in *M. truncatula* (Di et al. 2022), whereas RGF8 overexpression in *Arabidopsis* reduced lateral root number (Fernandez et al. 2015). This study showed significantly reduced lateral root density in *mttpst*, indicating that PSKs are the main sulfated peptides downstream of MtTPST that regulates lateral root formation in *M. truncatula*.

4.3 | MtTPST Regulates Nodule Initiation via Sulfated PSK

MtTPST was transcriptionally induced in *M. truncatula* roots by *S. meliloti* infection and showed markedly higher expression abundance in developing nodules relative to other organs and meristematic tissues, which strongly indicates that MtTPST is involved in nodule formation. The *promoter:GUS* staining revealed *MtTPST* to be expressed throughout the whole nodule developmental process, including in nodule primordia. Overexpression of *MtTPST* significantly increased nodule number in *M. truncatula*. Conversely, the *mttpst* mutant developed fewer nodules than wild-type plants, leading to reduced nitrogen fixation ability. Successful nodulation of legume roots depends on two early symbiotic events: rhizobial infection and nodule organogenesis (Oldroyd et al. 2011). Because *MtTPST* was highly expressed at the early nodule primordium, detailed observation of these early symbiotic events was performed, revealing that mutation in *MtTPST* caused a marked reduction in primordium number without affecting IT number. Conversely, overexpression of *MtTPST* in hairy roots increased primordium density while the IT formation was not affected. These findings prompt us to hypothesize that MtTPST positively regulates nodulation by promoting nodule initiation. Given the observation that *MtPSKδ* is highly expressed in nodule primordia and functions redundantly with PSK-α to induce nodule initiation (Yu et al. 2022), we treated *M. truncatula* seedlings with PSK-δ and RGF3 peptides. The results showed that only the sulfated PSK-δ partially restored nodule number in *mttpst*, indicating that PSKs, together with other untested sulfated peptide(s), function downstream of MtTPST to promote nodule initiation and primordium formation (Figure 9).

Interestingly, *MtTPST* expression was induced by rhizobial infection in wild-type *M. truncatula* but not in Nod factor signalling mutants. A similar expression phenomenon has also been reported for *MtPSKδ* (Yu et al. 2022). These findings indicate that MtTPST-PSK-δ module functions downstream of the Nod factor signalling pathway. Moreover, overexpression of *MtTPST* promoted nodulation in the wild-type *M. truncatula*

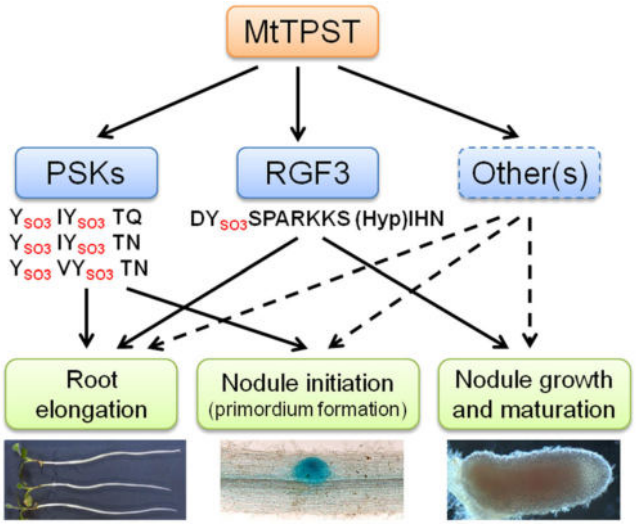

FIGURE 9 | Schematic model showing the functional mechanism of MtTPST. MtTPST catalyses tyrosine sulfation of PSKs (including PSK-α, PSK-δ and PSK-ε), RGF3 and other sulfated peptide(s) to achieve biological activities. The sulfated PSKs, combined with RGF3 and other peptide(s), coordinately promote root elongation, probably through regulation of root meristematic activity and cell elongation. PSKs and other peptide(s) act to induce nodule initiation to form nodule primordium, thereby increasing nodule number. RGF3, together with other peptide(s), positively regulates apical meristem activity to promote nodule growth and maturation. [Color figure can be viewed at wileyonlinelibrary.com]

but failed to induce nodule formation in *nfp* and *nin* mutants, suggesting that the upstream Nod factor signalling is strictly required for MtTPST-induced nodule formation.

Cytokinin and auxin are two critical regulators of nodule organogenesis (Liu et al. 2018; Lin, Frank, and Reid 2020). Transcriptomic and qRT-PCR analyses revealed that both cytokinin and auxin responses are involved in MtTPST-regulated nodule formation. Cytokinin is found to accumulate in the cortical cells of infected legume roots (Reid et al. 2017), which is consistent with our observation that both *MtTPST* and *MtPSK-δ* (Yu et al. 2022) expressions occur in the root cortex. Manipulating endogenous cytokinin level or its signalling remarkably affected symbiotic nodulation (Boivin et al. 2016; Dong et al. 2021). Specifically, overexpression of *LOG4*, a cytokinin-activating gene, in *L. japonicus* induced cortical cell division, leading to spontaneous nodule formation (Reid et al. 2017). In our results, expression of a *LOG* gene was downregulated in *mttpst* and was upregulated upon PSK peptide treatment. By contrast, a cytokinin-degrading gene *CKX* was transcriptionally upregulated in *mttpst* while application of PSK peptide repressed its expression. These findings indicate that MtTPST-PSK module promotes nodule initiation by positively regulating cytokinin accumulation. Auxin biosynthesis and signalling are of great importance for nodule initiation. Auxin predominantly accumulates in cortical cells undergoing division for nodule organogenesis (Suzaki et al. 2012), which is consistent with the expression pattern of *MtTPST* and *MtPSK-δ* at the same stage. Intracellular auxin may be modified by amino acid conjugation, leading to inactivation forms of the hormone. IAA-amino acid hydrolase ILR1 hydrolyze these conjugates to free IAA, thus increasing bioactive IAA accumulation (Korasick, Enders, and Strader 2013). We found that an ILR1-encoding gene was transcriptionally repressed in *mttpst*, but induced by PSK treatment of *mttpst*. Similarly, transcript levels of several auxin-responsive genes, including three SAURs, one ARF and three DRM1/ARPs (Hagen and Guilfoyle 2002), were significantly downregulated in *mttpst* and recovered by PSK peptide application. These findings prompt us to hypothesize that MtTPST-PSK promotes nodule initiation through inducing auxin accumulation and signalling. In addition, RNA-seq assay indicated that MtTPST-PSK might regulate downstream MAPK signalling pathway, with at least three MAPKKK genes were transcriptionally repressed in *mttpst*. It has been reported that both MAPK and MAPKK, the other two kinase components in MAPK signalling, are required for nodule formation in *L. japonicas* (Chen et al. 2012; Yin et al. 2019). Although few studies focused on their functions, MAPKKK proteins, which are important components of MAPK signalling pathway, should participate in nodulation regulation. Together, these results suggest a possible involvement of MAPK signalling in MtTPST-PSK-regulated nodule initiation.

4.4 | MtTPST Promotes Nodule Growth and Maturation by Sulfated RGF3

Furthermore, *MtTPST* expression was detected in the nodule apical meristem and the *mttpst* developed significantly smaller nodules than wild type, which was attributed to decreased nodule meristematic activity. These findings suggest that MtTPST promotes nodule growth and maturation by inducing meristematic cell proliferation. However, transgenic overexpression of *MtTPST* failed to promote nodule growth. The expression pattern showed that *MtTPST* transcript level is much higher in developing nodules than in other organs and tissues, which means it may have reached a saturated state in nodules. Therefore, in this situation, excess MtTPST activity produced by overexpression could not provoke additional phenotype. Similar to *MtTPST*, *MtPSKδ* and *MtRGF3* are both expressed in the nodule apical meristem (Li et al. 2020, Yu et al. 2022), indicating possible involvement of these two sulfated peptides in nodule growth. Nevertheless, exogenous application of the sulfated PSK-δ peptide had no obvious effect on *mttpst* nodule elongation, consistent with the finding that repression of *MtPSK* gene expression does not alter nodule size (Yu et al. 2022). In contrast, treatment with the sulfated RGF3 peptide, but not the unsulfated RGF3, significantly increased nodule size in *mttpst*, though it did not recover to the wild-type level, which indicates possible involvement of other sulfated peptide(s) in nodule growth. Given that RGF peptides are needed for maintenance of stem cell activity in roots (Matsuzaki et al. 2010), we propose that MtTPST-RGF3 signalling regulates meristematic cell proliferation to promote nodule growth and maturation (Figure 9).

Author Contributions

L.Y. conceived and designed the research. L.Y., D.Z., Q.D., and Q.L. performed the experiments. L.Y. and L.L. analyzed the data. K.S.M. and J.W. provided the mttpst mutant material. L.Y. wrote the manuscript. J.G. revised the manuscript. All authors read and approved the manuscript.

Acknowledgements

The authors thank Professor Ertao Wang at CAS Center for Excellence in Molecular Plant Sciences for kindly providing the *Medicago truncatula* nodulation mutants and thank Professor Jun Yang for critical discussion in manuscript revision. This study was supported by the National Natural Science Foundation of China (No. 31500197) and the State Key Laboratory of Subtropical Silviculture (No. SKLSS-KF2023-01).

Conflicts of Interest

The authors declare no conflicts of interest.

Data Availability Statement

All data supporting the findings of this study are available within the paper and within the supplementary data published online. The RNA-seq raw data are available in the NCBI Sequence Read Archive under the accession number PRJNA1121021.

References

Amano, Y., H. Tsubouchi, H. Shinohara, M. Ogawa, and Y. Matsubayashi. 2007. "Tyrosine-Sulfated Glycopeptide Involved in Cellular Proliferation and Expansion in *Arabidopsis*." *Proceedings of the National Academy of Sciences of the United States of America* 104: 18333–18338.

Benedito, V. A., I. Torres-Jerez, J. D. Murray, et al. 2008. "A Gene Expression Atlas of the Model Legume *Medicago truncatula*." *Plant Journal* 55: 504–513.

Boisson-Dernier, A., M. Chabaud, F. Garcia, G. Bécard, C. Rosenberg, and D. G. Barker. 2001. "*Agrobacterium rhizogene*s-Transformed Roots of *Medicago truncatula* for the Study of Nitrogen-Fixing and Endomycorrhizal Symbiotic Associations." *Molecular Plant-Microbe Interactions®* 14: 695–700.

Boivin, S., T. Kazmierczak, M. Brault, et al. 2016. "Different Cytokinin Histidine Kinase Receptors Regulate Nodule Initiation as Well as Later Nodule Developmental Stages in *Medicago truncatula*." *Plant, Cell & Environment* 39: 2198–2209.

Chen, T., H. Zhu, D. Ke, et al. 2012. "A MAP Kinase Kinase Interacts With SymRK and Regulates Nodule Organogenesis in *Lotus japonicus*." *Plant Cell* 24: 823–838.

Cosson, V., P. Durand, I. d'Erfurth, A. Kondorosi, and P. Ratet. 2006. "*Medicago truncatula* Transformation Using Leaf Explants." *Methods in Molecular Biology* 343: 115–127.

De Giorgi, J., C. Fuchs, M. Iwasaki, et al. 2021. "The *Arabidopsis* Mature Endosperm Promotes Seedling Cuticle Formation via Release of Sulfated Peptides." *Developmental Cell* 56: 3066–3081.e5.

Di, Q., Y. Li, D. Zhang, et al. 2022. "A Novel Type of Phytosulfokine, PSK-E, Positively Regulates Root Elongation and Formation of Lateral Roots and Root Nodules in *Medicago truncatula*." *Plant Signaling & Behavior* 17: 2134672.

Doblas, V. G., E. Smakowska-Luzan, S. Fujita, et al. 2017. "Root Diffusion Barrier Control by a Vasculature-Derived Peptide Binding to the SGN3 Receptor." *Science* 355: 280–284.

Dong, W., Y. Zhu, H. Chang, et al. 2021. "An SHR-SCR Module Specifies Legume Cortical Cell Fate to Enable Nodulation." *Nature* 589: 586–590.

Ferguson, B. J., C. Mens, A. H. Hastwell, et al. 2019. "Legume Nodulation: The Host Controls the Party." *Plant, Cell & Environment* 42: 41–51.

Fernandez, A., A. Drozdzecki, K. Hoogewijs, et al. 2013. "Transcriptional and Functional Classification of the GOLVEN/ROOT GROWTH FACTOR/CLE-Like Signaling Peptides Reveals Their Role in Lateral Root and Hair Formation." *Plant Physiology* 161: 954–970.

Fernandez, A., A. Drozdzecki, K. Hoogewijs, et al. 2015. "The GLV6/RGF8/CLEL2 Peptide Regulates Early Pericycle Divisions During Lateral Root Initiation." *Journal of Experimental Botany* 66: 5245–5256.

Fernandez, A. I., N. Vangheluwe, K. Xu, et al. 2020. "GOLVEN Peptide Signalling Through RGI Receptors and MPK6 Restricts Asymmetric Cell Division During Lateral Root Initiation." *Nature Plants* 6: 533–543.

Franssen, H. J., T. T. Xiao, O. Kulikova, et al. 2015. "Root Developmental Programs Shape the *Medicago truncatula* Nodule Meristem." *Development (Cambridge, England)* 142: 2941–2950.

Ghorbani, S., K. Hoogewijs, T. Pečenková, et al. 2016. "The SBT6.1 Subtilase Processes the GOLVEN1 Peptide Controlling Cell Elongation." *Journal of Experimental Botany* 67: 4877–4887.

Hagen, G., and T. Guilfoyle. 2002. "Auxin-Responsive Gene Expression: Genes, Promoters and Regulatory Factors." *Plant Molecular Biology* 49: 373–385.

Hanai, H., D. Nakayama, H. Yang, Y. Matsubayashi, Y. Hirota, and Y. Sakagami. 2000. "Existence of a Plant Tyrosylprotein Sulfotransferase: Novel Plant Enzyme Catalyzing Tyrosine O-Sulfation of Preprophytosulfokine Variants In Vitro." *FEBS Letters* 470: 97–101.

Igarashi, D., K. Tsuda, and F. Katagiri. 2012. "The Peptide Growth Factor, Phytosulfokine, Attenuates Pattern-Triggered Immunity." *Plant Journal* 71: 194–204.

Jones, K. M., H. Kobayashi, B. W. Davies, M. E. Taga, and G. C. Walker. 2007. "How Rhizobial Symbionts Invade Plants: the Sinorhizobium-Medicago Model." *Nature Reviews Microbiology* 5: 619–633.

Kaufmann, C., and M. Sauter. 2019. "Sulfated Plant Peptide Hormones." *Journal of Experimental Botany* 70: 4267–4277.

Komori, R., Y. Amano, M. Ogawa-Ohnishi, and Y. Matsubayashi. 2009. "Identification of Tyrosylprotein Sulfotransferase in *Arabidopsis*." *Proceedings of the National Academy of Sciences of the United States of America* 106: 15067–15072.

Korasick, D. A., T. A. Enders, and L. C. Strader. 2013. "Auxin Biosynthesis and Storage Forms." *Journal of Experimental Botany* 64: 2541–2555.

Kutschmar, A., G. Rzewuski, N. Stührwohldt, G. T. S. Beemster, D. Inzé, and M. Sauter. 2009. "PSK-α Promotes Root Growth in Arabidopsis." *New Phytology* 181: 820–831.

Ladwig, F., R. I. Dahlke, N. Stührwohldt, J. Hartmann, K. Harter, and M. Sauter. 2015. "Phytosulfokine Regulates Growth in *Arabidopsis* Through a Response Module at the Plasma Membrane That Includes CYCLIC NUCLEOTIDE-GATED CHANNEL17, H+-ATPase, and BAK1." *Plant Cell* 27: 1718–1729.

Li, Q., M. Li, D. Zhang, L. Yu, J. Yan, and L. Luo. 2020. "The Peptide-Encoding MtRGF3 Gene Negatively Regulates Nodulation of *Medicago truncatula*." *Biochem. Biophys. Res. Commun.* 523: 66–71.

Li, Y., Q. Di, L. Luo, and L. Yu. 2024. "Phytosulfokine Peptides, Their Receptors, and Functions." *Frontiers in Plant Science* 14: 1326964.

Limpens, E., C. Franken, P. Smit, J. Willemse, T. Bisseling, and R. Geurts. 2003. "LysM Domain Receptor Kinases Regulating Rhizobial Nod Factor-Induced Infection." *Science* 302: 630–633.

Lin, J., M. Frank, and D. Reid. 2020. "No Home Without Hormones: How Plant Hormones Control Legume Nodule Organogenesis." *Plant Communications* 1: 100104.

Liu, H., C. Zhang, J. Yang, N. Yu, and E. Wang. 2018. "Hormone Modulation of Legume-Rhizobial Symbiosis." *Journal of Integrative Plant Biology* 60: 632–648.

Lorbiecke, R., and M. Sauter. 2002. "Comparative Analysis of PSK Peptide Growth Factor Precursor Homologs." *Plant Science* 163: 321–332.

Love, M. I., W. Huber, and S. Anders. 2014. "Moderated Estimation of Fold Change and Dispersion for RNA-Seq Data With DESeq. 2." *Genome Biology* 15: 550.

Ma, Y., W. Zhu, W. Zhao, et al. 2023. "MtESN2 Is a Subgroup II Sulphate Transporter Required for Symbiotic Nitrogen Fixation and Prevention of Nodule Early Senescence in *Medicago truncatula*." *Plant, Cell & Environment* 46: 3558–3574.

Matsubayashi, Y. 2011. "Post-Translational Modifications in Secreted Peptide Hormones in Plants." *Plant Cell Physiology* 52: 5–13.

Matsubayashi, Y., and Y. Sakagami. 1996. "Phytosulfokine, Sulfated Peptides That Induce the Proliferation of Single Mesophyll Cells of *Asparagus officinalis* L." *Proceedings of the National Academy of Sciences of the United States of America* 93: 7623–7627.

Matsubayashi, Y., M. Ogawa, A. Morita, and Y. Sakagami. 2002. "An LRR Receptor Kinase Involved in Perception of a Peptide Plant Hormone, Phytosulfokine." *Science* 296: 1470–1472.

Matsuzaki, Y., M. Ogawa-Ohnishi, A. Mori, and Y. Matsubayashi. 2010. "Secreted Peptide Signals Required for Maintenance of Root Stem Cell Niche in *Arabidopsis*." *Science* 329: 1065–1067.

Meng, L., B. B. Buchanan, L. J. Feldman, and S. Luan. 2012. "CLE-Like (CLEL) Peptides Control the Pattern of Root Growth and Lateral Root Development in *Arabidopsis*." *Proceedings of the National Academy of Sciences of the United States of America* 109: 1760–1765.

Mohd-Radzman, N. A., and C. Drapek. 2023. "Compartmentalisation: A Strategy for Optimising Symbiosis and Tradeoff Management." *Plant, Cell & Environment* 46: 2998–3011.

Moore, K. L. 2003. "The Biology and Enzymology of Protein Tyrosine O-Sulfation." *Journal of Biological Chemistry* 278: 24243–24246.

Mortazavi, A., B. A. Williams, K. Mccue, L. Schaeffer, and B. Wold. 2008. "Mapping and Quantifying Mammalian Transcriptomes by RNA-Seq." *Nature Methods* 5: 621–628.

Mosher, S., H. Seybold, P. Rodriguez, et al. 2013. "The Tyrosine-Sulfated Peptide Receptors PSKR1 and PSY1R Modify the Immunity of *Arabidopsis* to Biotrophic and Necrotrophic Pathogens in an Antagonistic Manner." *Plant Journal* 73: 469–482.

Nakayama, T., H. Shinohara, M. Tanaka, K. Baba, M. Ogawa-Ohnishi, and Y. Matsubayashi. 2017. "A Peptide Hormone Required for Casparian Strip Diffusion Barrier Formation in *Arabidopsis* Roots." *Science* 355: 284–286.

Ogawa-Ohnishi, M., T. Yamashita, M. Kakita, et al. 2022. "Peptide Ligand-Mediated Trade-Off Between Plant Growth and Stress Response." *Science* 378: 175–180.

Okuda, S., S. Fujita, A. Moretti, et al. 2020. "Molecular Mechanism for the Recognition of Sequence-Divergent CIF Peptides by the Plant Receptor Kinases GSO1/SGN3 and GSO2." *Proceedings of the National Academy of Sciences of the United States of America* 117: 2693–2703.

Oldroyd, G. E. D. 2013. "Speak, Friend, and Enter: Signalling Systems That Promote Beneficial Symbiotic Associations in Plants." *Nature Reviews Microbiology* 11: 252–263.

Oldroyd, G. E. D., J. D. Murray, P. S. Poole, and J. A. Downie. 2011. "The Rules of Engagement in the Legume-Rhizobial Symbiosis." *Annual Review of Genetics* 45: 119–144.

Osipova, M. A., V. Mortier, K. N. Demchenko, et al. 2012. "WUSCHEL-RELATED HOMEOBOX 5 Gene Expression and Interaction of Cle Peptides With Components of the Systemic Control Add Two Pieces to the Puzzle of Autoregulation of Nodulation." *Plant Physiology* 158: 1329–1341.

Ou, Y., X. Lu, Q. Zi, et al. 2016. "RGF1 INSENSITIVE 1 to 5, a Group of LRR Receptor-Like Kinases, Are Essential for the Perception of Root Meristem Growth Factor 1 in *Arabidopsis thaliana*." *Cell Research,* 26: 686–698.

Pearce, G., D. Strydom, S. Johnson, and C. A. Ryan. 1991. "A Polypeptide From Tomato Leaves Induces Wound-Inducible Proteinase Inhibitor Proteins." *Science* 253: 895–897.

Reichardt, S., H. P. Piepho, A. Stintzi, and A. Schaller. 2020. "Peptide Signaling for Drought-Induced Tomato Flower Drop." *Science* 367: 1482–1485.

Reid, D., M. Nadzieja, O. Novák, A. B. Heckmann, N. Sandal, and J. Stougaard. 2017. "Cytokinin Biosynthesis Promotes Cortical Cell Responses During Nodule Development." *Plant Physiology* 175: 361–375.

Sauter, M. 2015. "Phytosulfokine Peptide Signalling." *Journal of Experimental Botany* 66: 5161–5169.

Shinohara, H. 2021. "Root Meristem Growth Factor RGF, a Sulfated Peptide Hormone in Plants." *Peptides* 142: 170556. https://doi.org/10.1016/j.peptides.2021.170556.

Shinohara, H., A. Mori, N. Yasue, K. Sumida, and Y. Matsubayashi. 2016. "Identification of Three LRR-RKs Involved in Perception of Root Meristem Growth Factor in *Arabidopsis*." *Proceedings of the National Academy of Sciences of the United States of America* 113: 3897–3902.

Song, W., L. Liu, J. Wang, et al. 2016. "Signature Motif-Guided Identification of Receptors for Peptide Hormones Essential for Root Meristem Growth." *Cell Research* 26: 674–685.

Stührwohldt, N., E. Bühler, M. Sauter, and A. Schaller. 2021. "Phytosulfokine (PSK) Precursor Processing by Subtilase SBT3.8 and PSK Signaling Improve Drought Stress Tolerance in Arabidopsis." *Journal of Experimental Botany* 72: 3427–3440.

Suzaki, T., K. Yano, M. Ito, Y. Umehara, N. Suganuma, and M. Kawaguchi. 2012. "Positive and Negative Regulation of Cortical Cell Division During Root Nodule Development in *Lotus japonicus* Is Accompanied by Auxin Response." *Development* 139: 3997–4006.

Truskina, J., S. Brück, A. Stintzi, et al. 2022. "A Peptide-Mediated, Multilateral Molecular Dialogue for the Coordination of Pollen Wall Formation." *Proceedings of the National Academy of Sciences of the United States of America* 119: e2201446119.

Wang, C., H. Yu, Z. Zhang, et al. 2015. "Phytosulfokine Is Involved in Positive Regulation of *Lotus japonicus* Nodulation." *Molecular Plant-Microbe Interactions* 28: 847–855.

Wang, J., H. Li, Z. Han, et al. 2015. "Allosteric Receptor Activation by the Plant Peptide Hormone Phytosulfokine." *Nature* 525: 265–268.

Wang, X., N. Zhang, L. Zhang, et al. 2021. "Perception of the Pathogen-Induced Peptide RGF7 by the Receptor-Like Kinases RGI4 and RGI5 Triggers Innate Immunity in *Arabidopsis thaliana*." *New Phytologist* 230: 1110–1125.

Whitford, R., A. Fernandez, R. Tejos, et al. 2012. "GOLVEN Secretory Peptides Regulate Auxin Carrier Turnover During Plant Gravitropic Responses." *Developmental Cell* 22: 678–685.

Xiao, T. T., S. Schilderink, S. Moling, et al. 2014. "Fate Map of *Medicago truncatula* Root Nodules." *Development* 141: 3517–3528.

Yamada, M., X. Han, and P. N. Benfey. 2020. "RGF1 Controls Root Meristem Size Through ROS Signalling." *Nature* 577: 85–88.

Yang, H., Y. Matsubayashi, K. Nakamura, and Y. Sakagami. 2001. "Diversity of *Arabidopsis* Genes Encoding Precursors for Phytosulfokine, a Peptide Growth Factor." *Plant Physiology* 127: 842–851.

Yang, J., L. Lan, Y. Jin, N. Yu, D. Wang, and E. Wang. 2022. "Mechanisms Underlying Legume-Rhizobium Symbioses." *Journal of Integrative Plant Biology* 64: 244–267.

Yin, J., X. Guan, H. Zhang, et al. 2019. "An MAP Kinase Interacts With LHK1 and Regulates Nodule Organogenesis in *Lotus japonicus*." *Science China Life Sciences* 62: 1203–1217.

Yu, L., Y. Liu, Q. Li, et al. 2016. "Overexpression of Phytosulfokine-α Induces Male Sterility and Cell Growth by Regulating Cell Wall Development in Arabidopsis." *Plant Cell Reports* 35: 2503–2512.

Yu, L., Q. Di, D. Zhang, et al. 2022. "A Legume-Specific Novel Type of Phytosulfokine, PSK-δ, Promotes Nodulation by Enhancing Nodule Organogenesis." *Journal of Experimental Botany* 73: 2698–2713.

Yu, L., H. Chen, J. Sun, and L. Li. 2014. "PtrKOR1 Is Required for Secondary Cell Wall Cellulose Biosynthesis in Populus." *Tree Physiology* 34: 1289–1300.

Zhang, H., Z. Hu, C. Lei, et al. 2018. "A Plant Phytosulfokine Peptide Initiates Auxin-Dependent Immunity Through Cytosolic Ca(2+) Signaling in Tomato." *Plant Cell* 30: 652–667.

Zhou, W., L. Wei, J. Xu, et al. 2010. "*Arabidopsis* Tyrosylprotein Sulfotransferase Acts in the Auxin/PLETHORA Pathway in Regulating Postembryonic Maintenance of the Root Stem Cell Niche." *Plant Cell* 22: 3692–3709.

Supporting Information

Additional supporting information can be found online in the Supporting Information section.